Tampere University

Nisatuz Jahra

STUDY AND ANALYSIS OF TEMPERATURE EFFECT ON IN-MOLD LABELED RFID TAGS

Master of Science Thesis
Wireless Communication
and RF Systems
1st examiner: Dr. Toni Björninen
2nd examiner: Dr. Jari Kangas
December 2021

ABSTRACT

NISATUZ JAHRA: Study and analysis of temperature effect on in-mold labeled RFID tags
Master of Science Thesis, 68 pages
Tampere University
Master's Degree Education in Electrical Engineering in
Wireless Communication and RF systems
November 2021

Radio frequency identification (RFID) technology is the most effective automated object identification solution in today's product markets. Among the enormous applications of RFID technology, In-mold labeled (IML) RFID tags are becoming very popular as it provides identification to the tags from the initial stage of production. In the manufacturing process of IML RFID tags, high-temperature melted plastic is injected into a mold where the RFID tag is placed beforehand. After injection, the plastic gets cold within a few seconds, and the product comes out with RFID tags in the shape of the mold. Due to this large temperature variation, the RFID tags get bumps or wrinkles. As a result of the uneven outlook, the customers reject these RFID tags, which is not cost-effective in production.

This study first attempts to find the root causes with the simulation and experiments to solve this problem. One possible reason for the wrinkled RFID tag can be uneven heat distribution on the antenna conductor. To verify this hypothesis, there are several steps have been taken including, (i) simulation of antennas, (ii) different mesh to decrease the conductor of the antenna without affecting its performance, (iii) prototyped antennas are tested with IML. The second potential cause of this problem is the inconsistency of the material properties (e.g., how a material behaves under high-temperature variation) of the multi-layer structure of the antenna. To verify the second hypothesis, different materials are used as antenna elements and substrates to overcome the wrinkling problem. The finalized antenna versions are sent to Tampere University's polymer laboratory to produce IML samples to analyze the solution.

As a result of this thesis, it is demonstrated that changing the antenna design has no influence on the temperature distribution of the IML process. Wrinkles emerge whether conductive materials are present or not. The key to resolving the wrinkling problem is to use the proper material type. Although the design adjustment has no influence on the wrinkling process, it becomes an environmentally friendly antenna with less conductive inks and a cost-effective solution.

Keywords: IML RFID tags, passive UHF RFID, conductive materials, read range, mesh pattens, screen printing

PREFACE

This thesis is provided by Avery Dennison Smartrac, Tampere, Finland, from May 2021 to December 2021. The IML trials have been done in Tampere University, Polymer laboratory, Faculty of Engineering and Natural Sciences.

First, I would like to thank Dr.Toni Björninen for his valuable instructions and guidelines for this thesis. I would be grateful to Dr. Elham Moradi for giving me the fantastic opportunity to become a part of this interesting topic. Special thanks to Dr. Shubin Ma for his kind support in teaching me the fundamentals of this work. Thanks to Dr. Tiina Vuorinen for contributing her excellency in material to this work and coming up with unique ideas. Also, I would be thankful to Dr. Katariina Penttilä for providing an innovative field to develop a dynamic research topic and all my colleagues at Avery Dennison Smatrac to make this thesis tenure memorable.

Finally, I want to convey my love and appreciation to my family, especially to my husband, who has provided constant support and encouragement.

Tampere, 07 December 2021

Nisatuz Jahra

CONTENTS

LIST OF FIGURES

LIST OF SYMBOLS AND ABBREVIATIONS

RFID	Radio frequency identification
IML	In-mold label
LF	Low frequency
HF	High frequency
VHF	Very-high frequency
UHF	Ultra-high frequency
IoT	Internet of things
QR	Quick response
EPC	Electronic product code
GID	General identifier number
ID	Identifier
IC	Integrated circuit
PET	Polyethylene terephthalate
EM	Electromagnetic
RHCP	Right Hand Circularly Polarized
LHCP	Left Hand Circularly Polarized
PLF	Polarization Loss Factor
FEM	Finite element method
CFD	Computational fluid dynamics

1. INTRODUCTION

1.1 Background

Since it started at the beginning of the twentieth century, radio-frequency technology has advanced significantly. In 1946, a Russian scientist named Leon Theremin is largely credited with creating the first RFID device, which is the first successful RFID application [1].

Radio Frequency Identification (RFID) is used to track and identify any objects with RFID tags attached to them. Due to the facility of monitoring and tracking, RFID is becoming a vital tool in all sectors such as; medicine, food supply, retailer, vehicle control. RFID technology is slowly developing a strong presence in the product packaging industry. Large corporations, including Wal-Mart, Tesco, and the US Department of Defense [2], are dedicated to using this technology across open supply chains. The focus has changed from initial stages and lab testing to widespread implementation across the world [3]. The advantages of RFID technology over previous identifying systems, as well as the advent of microelectronic technology in the 1970s, have contributed to its further growth [4].

RFID is a combination of radar and radio transmission. Radar was invented in the United States in the 1920s. In the nineteenth century, scholars realized the relation between electricity and magnetism, which is the foundation of radio transmission [5]. In 1948, Harry Stockman published a landmark article outlining the possibility of modulating a target's radar signature for the purpose of data communication. However, he noted the massive amount of research and development required before the communication by means of reflected power could be utilized in applications [6]. Gradually, this led to the development of today's RFID technology. First, it started to become popular in libraries, transportation, business, and theft-monitoring systems [7]. As a result of the advancement of RFID applications, it may benefit substantially from its widespread adoption. Figure 1 illustrates a brief revolutionary history of RFID technology [6].

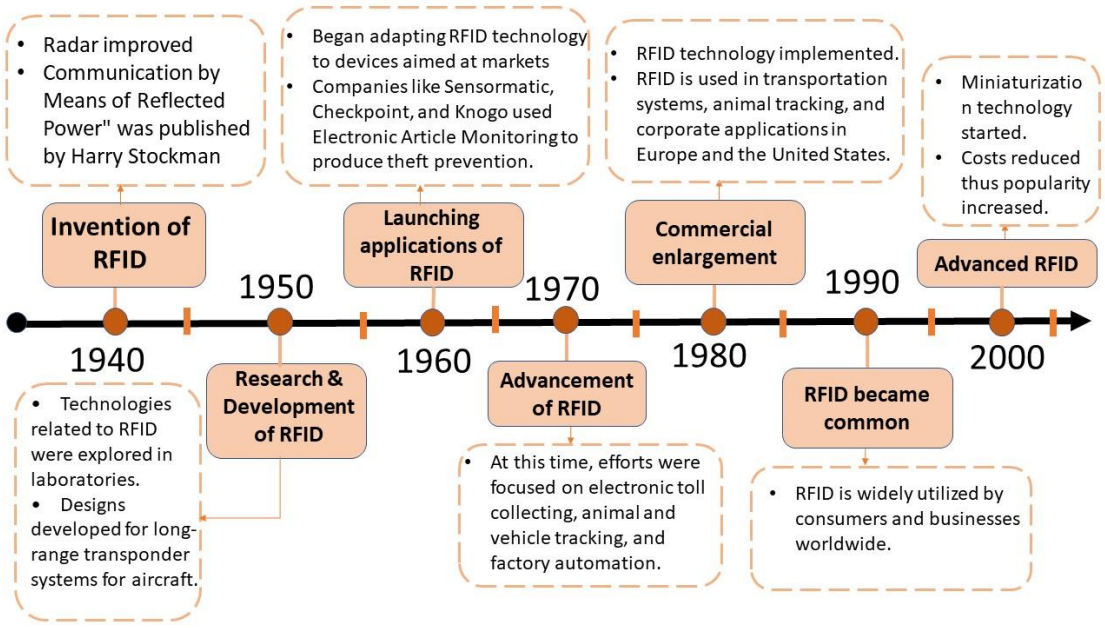

Figure 1. *Evolution of RFID technology*.

RFID technology coupled with sensor components that collect environmental characteristics, in addition to the identification, is becoming increasingly important in the context of smart things, the Internet of Things (IoT) or Industry 4.0. RFID tags are important in smart industry concepts as they can provide battery-free temperature, pressure, proximity, and humidity readings [8].

RFID tags operate in different frequencies; low frequency (LF), high frequency (HF), ultra-high frequency (UHF) [9,10]. UHF and HF are two categories related to use near water or in food products containing water. The data transfer rate between the tag and the reader is slow with the HF tag, but the data transfer rate between the tag and the reader is very fast with the UHF tag [9,10]. UHF tags are popular due to their smaller size and higher performance rating [3]. The operating frequencies of RFID tags are discussed in chapter 2 (section 2.1.1).

From product labeling to extensive wireless sensing, UHF passive radio-frequency identification technology applications are quickly advancing in different industries. A large number of scientific studies show that the physical attributes of an object can be observed and monitored remotely throughout its entire lifecycle using UHF RFIDs. Recently, advancements in the size and cost of passive UHF RFID tags as well as their broad usage in the supply chain, retail, and government sectors, have resulted in increased use of passive UHF RFID tags compared to decades before. RFID has the following advantages: very big ID numbers (usually 96 bits) allow each item to have a unique ID; fast identification of huge numbers of tags, which is helpful for mechanically scanning cases on pallets; does not require line of sight. Thus, tags may be encapsulated

or concealed while still being read; security elements, such as password-secured operations, make RFID a more secure technology. Based on a well-known standard, there has been widespread acceptance across the world. UHF passive RFID tags with UHF sensing capabilities may be the fascinating research trend, with substantial implications for the Internet of Things (IoT). A clear understanding of a technology's capabilities and limits is essential for the community [11][12].

In [13], the authors have shown that RFID tag performance degrades a lot when it comes into contact with metal or water. According to them, generally, larger tags perform better, with smaller tags doing much worse than the 4-in tags. 867 MHz also has comparable performance in free space, near metal and water. However, near metal and water has a dramatically decreased performance. According to early research, UHF near-field tag performance does not overcome the metal/water problem, and in fact, declines more substantially than far-field tags. As well, it was shown that the tag-reader system is reverse-link restricted in terms of the readers. The IC reacts, but the reader cannot detect it. The communication range between the reader and the tag is explored in [14]. They designed a passive UHF RFID prototype system to increase the communication range. Their prototype used an intermittent transmission mechanism that reduces the power consumption of IC. Their findings reveal that adopting discontinuous transmission with a duty ratio of 40% reduced power usage by three-quarters. This paper shows that optimizing the sending signal can reduce tag IC power consumption while also boosting communication range.

In a globalized society, commodities' movements are complex and comprised of various procedures involving various agents, including the providing company, the distribution company, the receiving company, various customs agencies, transportation firms, and so forth. It is obvious that all these activities must be coordinated to maximize time and resources. Simultaneously, it must ensure the safety of commodities and consumers. In this case, RFID-enabled automated management shines for its capabilities and benefits. The flow of products is simplified and improved with complete dependability, thanks to the automation of RFID tags.

Nowadays, RFID has become one of the most reliable ways to track and identify products. RFID tags can be used to tag products of varying sizes and categories. Identifying products is part of inventory management which is one of the most important things for companies. Due to this benefit, the companies are more invested in RFID technology which in turn creates a great market potential for the RFID tags research [15].

As a result, item level labeling has a substantial financial incentive. Aside from the economic advantages, labeling individual items will enable intelligent packing and shelving. This is a significant benefit for the food or medicine sector and garments sector. The benefits of tracking and tracing all tags will be represented at the item, but there is also the ability to recognize expired products on the shelf and to be able to remove these products before customers can purchase them, creating an optimal environment for product branding for both retailers and manufacturers. Those investing in product-level tag adoption can now expect hefty returns as the technology takes off, with 550 billion items expected to be tagged in 2016 [15].

RFID in packaging or in a plastic product requires an injection molding process. Injection molding is a plastic shaping technique that uses high temperatures and pressures. It is a technique in which molten plastic is injected through a tiny hole, known as the injection point, to fill a cavity system that will eventually become the package [16]. After the molten plastic cools, the cavity system opens, and the part is removed. The mold design must allow components to be ejected; for example, the walls should have a slight slope for easy dispensing. If the sidewall of the container is too straight and deep, the part may not be ejected properly, which will impair the efficient speed of operation [16-19]. During the manufacturing process, the in-mold label RFID tag is applied to the container/items. Preprinted labels are fed into the mold and are an essential component of the finished item, eliminating the need for equipment to apply labels to the fill line.

In-mold labeling (IML) is applied to inflatable containers or bottles made of polyethylene or polypropylene. The label substrate can be paper, which is coated with a heat-sensitive adhesive, or a film such as polypropylene, which adheres directly to the blow molding case. In some instances, retailers are requesting that top suppliers put RFID tags to injection molded goods containers and pallets. Certain packing materials reflect radio signals, while others absorb them. Injection molding is a cost-effective production method, especially for the large-scale production of intelligent plastic components with integrated RFID tags. The following part explains the problem statement of this thesis related to IML RFID tags.

1.2 Problem identification and possible solutions

During the IML process, melted plastic of a very high temperature is injected on the RFID tag; then, it cools down when the mold is filled up by plastic. This process happens within a very short time, and during this time, the RFID tag goes through very high-temperature variance. Usually, after this process, the RFID tag comes out with wrinkles or bumps on

it [17-19]. In figure (2) shows such an RFID tag after in-mold labeling contains wrinkles on it.

Figure 2. *Wrinkled RFID tag after IML process.*

The RFID tags are always hidden behind a face material or cover to hide the antenna design in commercial uses. When the antenna gets wrinkled under the cover, it will also be visible on the face material. This is a very common problem of such a tag, getting wrinkles or bumps after the IML process. Due to this issue, a massive amount of functional RFID tags gets discarded due to aesthetic reasons, reducing the cost-effectiveness of the production.

The objective of this study is to find out an effective solution to this mentioned problem. Initially, the aim was to justify the solution by changing the antenna design. It was assumed that the wrinkles might happen due to uneven heat distribution on the conductive materials of the antenna elements. The first idea was to reduce the amount of conductive material from the antenna so that, with less amount metal or conductive inks, the surface gets less heated, and there will be fewer possibilities of getting wrinkles. Additionally, the antennas were fabricated in the same design in different materials to see the effect of materials in the IML process. Lastly, all the samples were tested through the IML process at Tampere University, polymer laboratory (Faculty of Engineering and Natural Sciences), to analyze the outcomes. Two different prototype antennas provided by Avery Dennison are used for the experiment.

1.3 Structure of the thesis

The basic ideas related to the topic are discussed in chapter 2. In this chapter, fundamental topics of RFID and essential parameters of antenna are discussed elaborately. Also, a brief description of injection molding is given to provide the reader with an overall idea of the topic. Chapter 3 describes the procedures to execute the entire experiment.

This chapter has several sections containing each step of the analysis. Chapter 4 discusses the results of the experimental and simulated outcomes. As the procedures are divided into several parts, the results are also segmented to provide a clear conception and to keep the analysis simple. The result section includes all the simulation and measurement results and is discussed extensively. Pictures are also represented to visualize the outcomes of the IML trials. Through the experiments, the resultant solution has been identified. In the results section, all these observations are done sequentially. Finally, chapter 5 represents the limitations that appeared through the execution of the experiments. This chapter discusses the conclusion, limitations, and future scope of this work.

2. LITERATURE REVIEW

2.1 Radio frequency identification (RFID) technology

A typical RFID hardware system includes a reader device or transponder that collects data from RFID tags, a reader antenna that converts electrical currents into electromagnetic fields, and RFID tags that hold unique information [8]. The RFID tag or inlay that is attached to any object receives the radio wave transmitted from the readers and reflects the signal to the antenna. The signal that returns from the tag carries the product information to the computer that is associated with the reader, where the information can be viewed on the screen and validated [2]. Figure 3 illustrates the basic structure of RFID communication. The reader antenna transmits the signal to the RFID tag, and the reflected signal from the tag comes back to the reader to show the product details in the host computer.

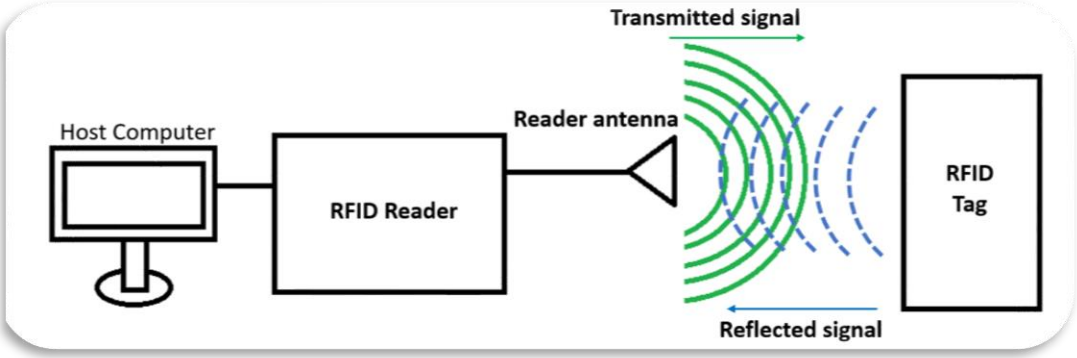

Figure 3. *The basic architecture of RFID technology*

In comparison to currently utilized optical technologies like Quick Response (QR) or Data Matrix Codes, communication between an antenna-equipped RFID reader and one or more passive, semi-active, or active RFID tags facilitates readability during applications without visual accessibility. Furthermore, RFID technology provides advantages such as simple bulk data collecting, the ability to combine numerous sensors (sensor tags), better memory capacities, and plagiarism prevention. Reduced pricing for RFID transponders in recent years has enabled a variety of economically viable uses, particularly in logistics.

The Electronic Product Code (EPC) is a universal and definitive identifier for things used in logistics, as are the GS1 identifying keys such as the Global Trade Item Number (GTIN) or the General Identifier Number (GID) (GI). In the context of smart products, the Internet of Things, or Industry 4.0, RFID technology combined with sensor components

for environmental parameter gathering is becoming increasingly crucial. 4.0. Passive RFID sensor tags enable battery-free temperature, pressure, proximity, and moisture measurements [8].

Typically, RFID readers use either monostatic or bistatic antenna configuration. In the monostatic configuration, a single antenna is responsible for the transmission and reception. In the bistatic configuration, two collocated antennas are used separately for transmission and reception. Readers using bistatic antennas tend to achieve better sensitivity. In this configuration, two separate antennas are used for transmitter and receiver. As a result of using separate antennas, they provide better electromagnetic isolation between transmitting and receiving circuit branches within the reader device [20].

2.1.1 Types of RFID

In terms of frequency, RFID tags have three categories: Low frequency (LF, 30 – 500kHz), High frequency (HF, 10 – 15MHz), Ultra-high frequency (UHF, 850 – 950MHz, 2.4 – 2.5GHz, 5.8GHz) [21]. Whether the tag is LF, HF, or UHF, it must stay within the reader's range to be functional, meaning the reader must receive the signal, and the tag must be able to transmit it back. Usually, low-frequency tags operate between 125 to 134.2 kHz and 140 to 148.5 kHz [21]. LF tags have the benefit of being unaffected by liquids or metals. On the other hand, the short-read range of these RFID tags is a drawback. HF tags are more expensive than low-frequency tags, but they have better transmission rates and longer ranges. This category is dominated by smart tags, which operate at a frequency of 13.56 MHz [21].

UHF tags are employed to remedy the limited read range; among all types of tags, UHF tags have the greatest range. Passive tags have a range of 3-6 meters, whereas active tags have a range of 30 meters or more [21]. Furthermore, the UHF tag allows the reading of a single tag in a brief period of time. For items that move fast and only stay within range of a reader for a short time, this functionality is essential. Because of these characteristics, UHF is most used in automated toll collecting systems. 868 MHz (Europe), 915 MHz (USA), 950 MHz (Japan), and 2.45 GHz are common frequencies. UHF tag frequencies vary by region and require a permit. UHF tags are more expensive than other tags, and fluids and metal have a negative impact on them. That is why most RFID applications may be built with LF tags since they are unaffected by liquids or metals, do not require a license, and can be used globally [21].

In terms of power or energy, there are three sorts of RFID tags: passive, semi-passive, and active tags. Firstly, passive tags do not have an internal power source and rely on the power induced by the reader. This means the reader must maintain its field until the

transaction is finished. These tags are the smallest and cheapest tags available because of the lack of a battery which increases their lifespan notably.

The second form of RFID tag is semi-passive. The microchip in those tags is always powered by an internal power source. There are other benefits; because the chip is always powered, it can react to queries faster, increasing the number of tags queried per second, which is critical in some applications. Furthermore, because the antenna isn't used for gathering power, it can be tuned for backscattering, extending the reading range. Finally, because the tag does not draw energy from the field, the backscattered signal is stronger, extending the range even further. For these reasons, a semi-active tag has a range that is normally greater than a passive tag. Finally, active tags are the third sort of tag. They have an internal power source, just like semi-active tags, but they utilize the energy to power the microprocessor as well as generate a signal on the antenna. Beacons are active tags that broadcast signals without being queried. Their range can be tens of meters, making them suitable for locating items or functioning as landmarks. The lifespan can be up to 5 years [21].

There are many kinds of far-field RFID reader antennas; the most common ones are circularly polarized antennas for tags that are orientated randomly. In the case of the fixed orientation of the tag's linear antennas (such as dipole antennas) have been used. Far-field antennas which have satisfactory performance over the UHF RFID band of 840−960 MHz (13.3 percent) would be desired for different applications [22]. In far-field systems, the reader and the tag communicate through the radiated electromagnetic plane waves in free space. The far-field tag antenna is typically a dipole half a wavelength long and thus frequency-dependent. The half-wavelength dipole is to conjugate match to the IC impedance and to get efficient radiation from the antenna. The smaller the far-field RFID antenna, the higher the frequency [23].

Usually, LF and HF RFIDs are near-field antennas. Inductively coupled Loop antennas have been commonly used as readers in LF/ HF systems. In inductive coupling, the reader and the tag communicate mostly via the magnetic field. These systems are mostly used in different applications like the magnetic field stores the majority of the reactive energy. This system has the advantage of operating in metal and liquid environments—however, materials with strong magnetic permeability influence such systems.

On the other hand, capacitive coupling devices have the disadvantage of being significantly influenced by objects with high dielectric permittivity as the energy is stored in the electric field. Therefore, it is not preferred to use capacitive coupling in real applications

[24]. The loop antenna is not enough to operate in the UHF band in most cases, as the standard solid-line loop antenna cannot offer adequate coverage. In some papers, the solution of UHF near the field has been presented. In [24], they have implemented a loop antenna which provides a very strong and evenly distributed magnetic field for broad-band UHF near-field RFID applications.

2.1.2 RFID tag manufacturing

As tags are used in large quantities in the supply chain and have a short functional life, they must be inexpensive. As a result, very basic antenna designs such as dipoles emerge. Furthermore, because the 4-in label is an industry-standard [20], most dipole antennas are meandering to be less than 4 in overall length. The most typical widths are 1/2 and 1 inch; however, various sizes are available. The construction of an RFID tag has several steps which need to be performed very precisely. The fabrication of the tag antenna process for tags entails etching a tag antenna from metals or using conductive inks. Antennas are frequently formed of copper, aluminum, or silver ink, and a variety of low-cost materials and manufacturing techniques are available. Antennas are usually bonded to a PET film substrate, which makes the tag flexible [20].

The inlay can be formed after the antenna has been created by attaching the antenna and IC. Attaching the IC gives the antenna the excitation port to conduct current flow in it. This step must be performed very efficiently, the IC and antenna should be properly positioned. To have a working inlay, the antenna must first be placed on the substrate, and then the chip must be placed in a very precise location. The IC attachment can be done by direct attaching method or using external straps. In direct attachment in IC is picked and placed onto an antenna, and conductive adhesives are used to attach the two items to the substrate. In the strap attachment method, the IC is first attached to an external strap which is then conductively adhered to the antenna and inlay substrate. This technique is much faster than the other process, allowing for reel-to-reel manufacturing and requiring much less precision of placement; however, it has the disadvantage of adding a small amount of thickness to the inlay [6].

2.2 Antennas for UHF RFID tags

An antenna is a transducer that transforms electrical power into electromagnetic waves and vice versa. An antenna can be used as either a transmitting or receiving antenna. The transmitting antenna transforms electrical impulses into electromagnetic waves and transmits them. On the other side, the receiving antenna transforms electromagnetic waves from a received beam into electrical impulses. The same antenna can be used

for both transmission and reception in two-way communication. The electrical power is related to the signals confined within the transmitter and receiver. On the contrary, the EM energy radiates unboundedly to the surrounding space according to the radiation pattern of the antenna.

RFID antennas provide two essential functions. The antennas initially enable the RFID tags to transmit electricity to them and when it receives data from the active tags. At the same time, a single antenna may enable and receive data from many tags. When the antenna is switched on, it generates a cloud of radio frequency (RF) radiation. RFID tags discovered in this cloud will be activated and scanned. This is often known as the tag read. The size and form of the field vary based on the kind and design of the antenna. The antenna design will also define the performance (e.g., read range, directivity, gain, efficiency, etc.) of the RFID tag.

Depending on the application requirement, the type of antenna to be used is different. There is no unique design of antenna that can be utilized for every purpose. Usually, different RFID tags might use the same microchip/IC, but every design will have specific features depending on the application.

One of the most common types of antenna is the half-wavelength dipole antenna. The fundamental implementation of this type of antenna is simple, and many of the basic computations can be done using closed-form approximation formulas. A basic dipole antenna works on the HF, VHF, and UHF parts of the radio frequency spectrum. The receiver or transmitter is normally connected to the dipole antenna through a feeder line, which allows power to be transmitted from one place to another. Many of the dipole antenna's characteristics are determined by the length of the radiating components, including its current distribution, input impedance, and radiation pattern [25]. Figure 4 shows the basic structure of the half-wavelength dipole antenna.

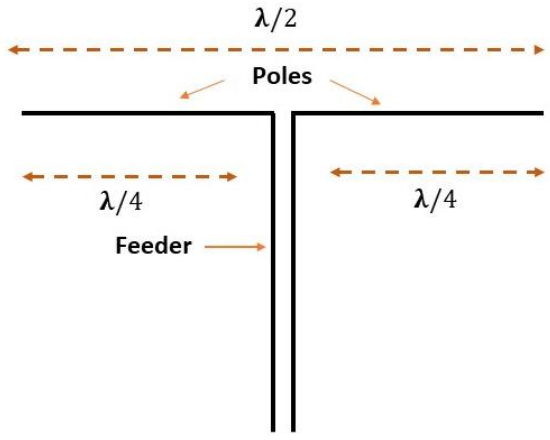

Figure 4. *Basic structure of a half-wavelength dipole antenna*.

The term ' half-wavelength refers to the fact that a dipole antenna is consists of two poles or conductors with a total length of half of the wavelength (λ/2). The conductors are placed on the same axis, and each pole on both sides has a length of a quarter of the wavelength (λ/4). The reason for this kind of construction is to get efficient radiation and make the antenna resonant. The feeding point generates current in the antenna poles and flows through the conductors in the back and forth direction. One wavelength means a complete cycle in a unit time. The time taken for an AC Waveform to complete one full pattern from its positive half to its negative half and back to its zero baseline again is called a Cycle and one complete cycle contains both a positive half-cycle and a negative half-cycle. The induced current is alternating; therefore, the cycle continues accordingly. This alternating oscillation enables the antenna to cancel the reactance of the half-wavelength antenna and it becomes fully resistive to resonate (more details in section 2.2.1). If the length of the conductor is λ, then each pole produces one half-cycle alternating current. As this continuous current contains an opposite direction, they cancel out each other, and no radiation happens. Therefore, the half-wavelength dipole is effective in getting sufficient radiation. Figure 5 shows the current of the half-wavelength dipole antenna. The current is zero at the end of the dipoles and maximum at the feeding point in the case of one-wavelength dipole.

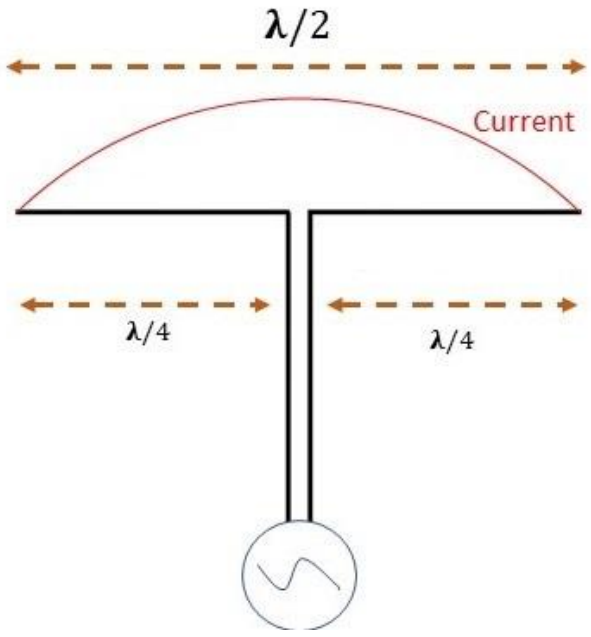

Figure 5. *Current in a half-wavelength dipole antenna*.

In the case of RFID antennas, the feeder line is the microchip or IC. The impedance matching is the most important characteristic of dipole antennas. The impedance of the RFID antenna and the IC must match to establish a connection between reader and tag.

Meandered line antennas are extensively used antennas in different RFID applications. These antennas are wire antennas with a specific length of wire but folded in multiple layers to reduce the overall dimension of the antenna. The resonant frequency can be decreased or increased by optimizing the wire length.

The wire antenna radiation depends on the features such as length, and radius of the wire, antenna design, the total dimension (length, width, and thickness) of the antenna structure, amount of the surface area. In meandered antennas, the wires are folded in small sections, and the current flow directions change close to each other. If two small wires are aligned closely to each other and turn in the opposite direction, the current flow tends to cancel, resulting in reduced resonant frequency. On the other hand, if the wires are closely aligned in the same direction, the current reunites and boosts the resonant frequency. This is how rearranging the turns of the direction or number of folds can optimize the desired resonant frequency in meandered antennas [26]. By meandering, a wire antenna can be shortened by 25 - 40% [27].
Figure 6 shows an example of a meandered antenna. The tuning of this type of antennas is straightforward by trimming off the metal parts or changing the number of folds [28]. Figure (6) shows an example of a meandered dipole antenna.

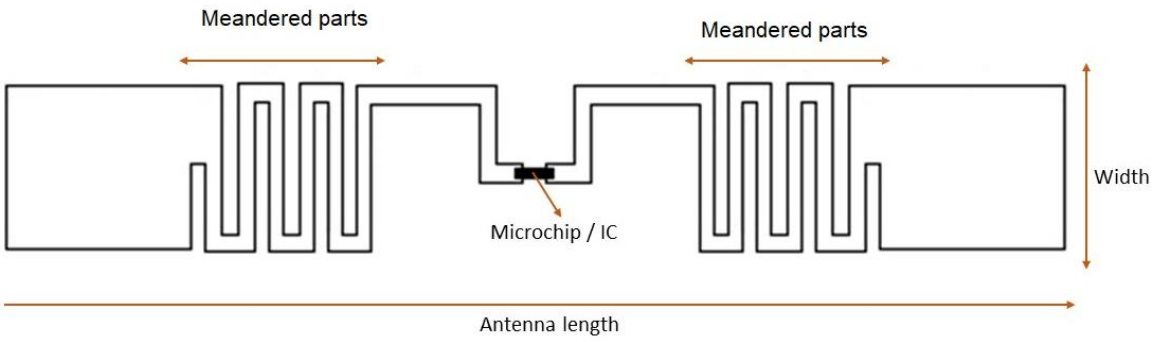

Figure 6. *An example of a meandered dipole antenna*.

2.2.1 Impedance and Impedance Matching

Impedance represents the ratio of voltage to current at an antenna's terminals. Impedance is the summation of the real and imaginary components of the antenna. characterizes the antenna's impedance as

$$Z_a = R_{ant} + jX_{ant} \tag{1}$$

where R_{ant} is antenna resistance at terminals, and X_{ant} is antenna reactance.

The impedance of an antenna is frequency-dependent. The antenna impedance can be approximated with closed-form equations only in very simple cases, such as a half-wave-length wire dipole. The antenna resistance consists of two components; that is

$$R_a = R_r + R_L \tag{2}$$

where R_r is the antenna's radiation resistance, and R_L is the antenna's loss resistance. The loss resistance represents ohmic loss arising from the materials the antenna is made up of, including the materials it interacts with through near-field coupling. The antenna's radiation resistance is determined by the antenna's shape and materials [29]. By definition, when the antenna's terminals are powered, R_r dissipates the same amount of power as the antenna's radiated power P_r.

Complex conjugate impedance matching is crucial for providing maximum power transfer [29]. It is used to maximize power transmission between the source and load. To transfer the maximum amount of power, the source and load impedance should be complex conjugate to each other. When the load and source resistances are equal, and load reactance equals the negative of the source reactance, then the maximum power transfer occurs.

An RFID tag is represented in the following circuit (in figure 7) to show the complex conjugates of antenna and IC impedances. The figure illustrates that antenna impedance is $Z_{ant} = R_{ant} + jX_{ant}$ and IC impedance is $Z_{ic} = R_{ic} + jX_{ic}$. The antenna acts as a source, and the antenna designer needs to tune it to the complex conjugate of the chip. So that, $R_{ant} = R_{ic}$ and $X_{ant} = -X_{ic}$.

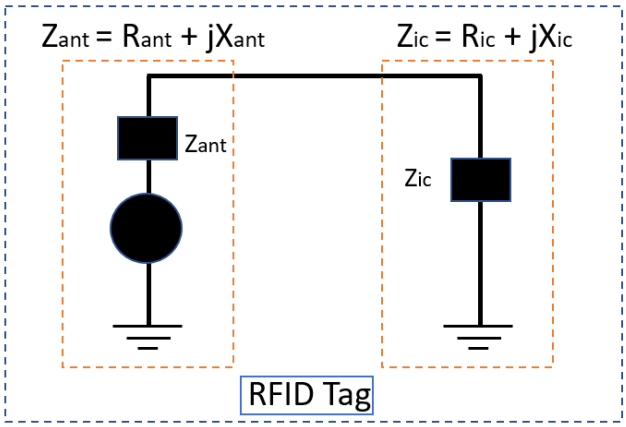

Figure 7. *Circuit representation of an RFID tag.*

Referring to the diagram in Fig. 7, the power received by the IC is represented as [30]

$$P_{IC} = \tau P_{ant} \tag{3}$$

In this equation, P_{ant} is the power received by the tag antenna from the reader and τ is the power transmission coefficient given by [40]

$$\tau = \frac{4R_{ant}R_{IC}}{|Z_{ant}+Z_{IC}|^2}. \quad (4)$$

The RFID IC impedance is frequency-dependent and capacitive. It is often modeled as a parallel connection of an equivalent resistance (R_{eq}) and capacitance (C_{eq}) as

$$Z_{ic} = \frac{1}{\frac{1}{R_{eq}}+j2\pi f C_{eq}}. \quad (5)$$

For the tags with strap attached IC, the IC impedance comprises an additional capacitance (C_{strap}) due to the strap fixture:

$$Z_{ic} = \frac{1}{\frac{1}{R_{eq}}+j2\pi f\left(C_{eq}+C_{strap}\right)}. \quad (6)$$

2.2.2 Antenna radiation parameters

Antennas are the most important part of RFID technology. Whatever the type or shape of the antenna is, some parameters are always important to consider. This section describes such parameters of an antenna.

Radiation efficiency

The ratio of the radiated power to the provided input power is known as radiation efficiency (e). Radiation efficiency can be expressed as,

$$e = \frac{\text{Prad}}{\text{P(input)}} \quad (7)$$

Most of the power from the transmitting antenna radiates if it has high efficiency. On the other side, maximum power is absorbed as losses inside the antenna or reflected away owing to impedance mismatch in a low-efficiency antenna (discussed in section). [31].

The ratio of the power given to the radiation resistance Rr to the power delivered to the radiation resistance Rr and the loss resistance RL is also known as radiation efficiency. The radiation efficiency can also be written as [4]

$$e = \frac{R_r}{R_r+R_l} \quad (8)$$

Directivity and Radiation pattern

The ratio of the highest radiation intensity in the primary beam of the antenna to the average radiation intensity throughout all space is described as directivity (D). The radiation intensity is expressed in (W/rad). Directivity is defined by,

$$D = \frac{\text{U max}}{\text{U average}} \ (dB) \tag{9}$$

where, U is the radiation intensity.

An antenna's directivity is equal to the ratio of its radiation intensity in a given direction to that of an isotropic source. The total power radiated (Prad) by the antenna divided by 4π is the average radiation intensity. So, equation (9) can be represented as [32]

$$D = \frac{\text{U max}}{\text{U average}} = \frac{4\pi\ \text{Umax}}{\text{Prad}} \tag{10}$$

The radiated power per unit (power density) of an Isotropic antenna is equal in all directions. At every distance from an isotropic antenna, the power density is just the transmitter power divided by the surface area of a sphere at that distance. If the area of the sphere is $4\pi R^2$, where R is the radius of the sphere, the power density P(density) in per unit (W/m^2) is,

$$\text{P(density)} = \frac{\text{P (transmitted)}}{4\pi R^2}\ (\text{W/m}^2) \tag{11}$$

Isotropic antennas are imaginary ideal antennas. In practical cases, antennas have certain directions where they radiate power over specific surface areas. For directional antennas, If the transmitting antenna has gain G_t ,the power density can represent as,

$$\text{P(density)} = \frac{\text{P (transmitted)} * \text{Gt}}{4\pi R^2}\ (\text{W/m}^2) \tag{12}$$

From equation 3, power density can relate to the source power or transmitted power, P_s,

$$\text{P(density)} = \frac{\text{Ps} * \tau\ \text{Gt}}{4\pi R^2}\ (\text{W/m}^2) \tag{13}$$

Antenna gain is described in the following parts of this section.

A single antenna cannot radiate isotopically. So, generally, antenna can not emit equally in all directions. In order to establish the radiation characteristics of an antenna in different angles or directions, a radiation pattern is always required [33]. If the antenna is set at its origin, the radiation pattern is a three-dimensional graph representing the radiated power of the antenna as a function of azimuth ($\boldsymbol{\Phi}$) and elevation ($\boldsymbol{\theta}$) angles.

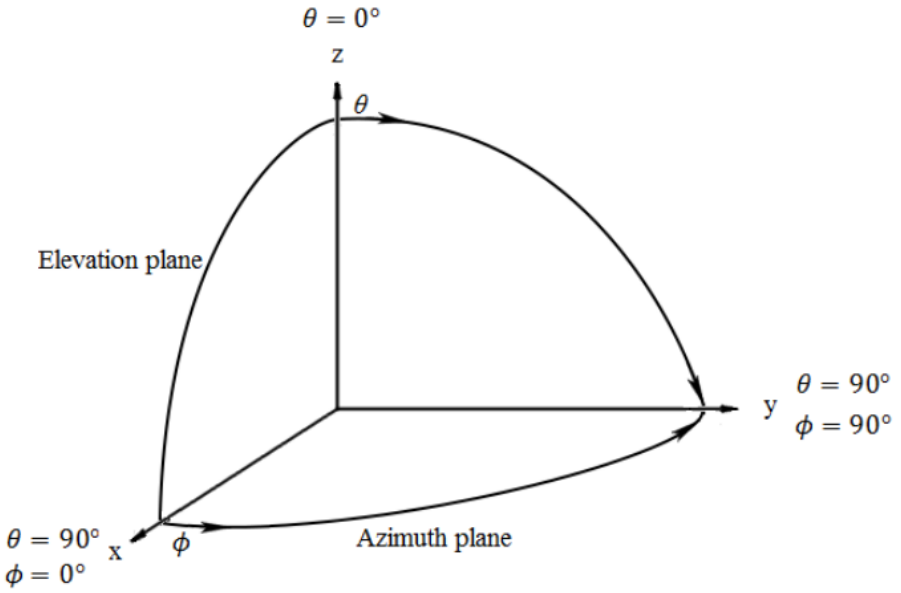

Figure 8. *Polar coordinates of an antenna [4].*

It's possible to identify distinct radiation lobes in a radiation pattern, each of which has its own maximum. The main beam of the antenna has the highest value, and the side-lobes have lower values. Radiation patterns also provide the antenna's 3dB angular beam width. If the main beam of an antenna is broad, it can transmit/receive signals over an extensive area, whereas a narrow main beam antenna can transmit/receive power over a limited area. In the main beam, the power density of radiated wave reduces by 3 dB [4]. Figure 9 shows an example of a three-dimensional radiation pattern of a half-wavelength dipole antenna.

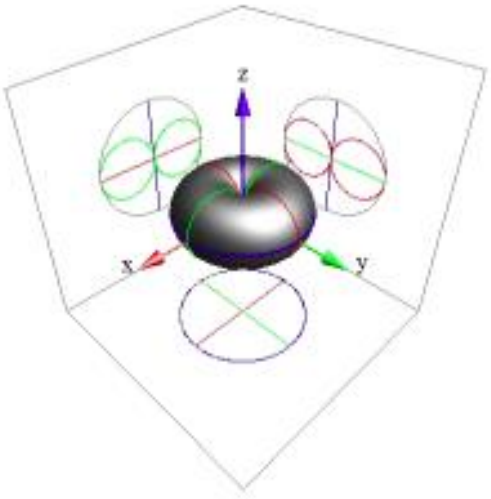

Figure 9. *Three-dimensional radiation pattern of an half wavelength dipole antenna [4].*

Gain

Antenna gain is defined as the product of directivity and efficiency. Gain and directivity of an antenna are functions of angles theta and phi. The gain of an antenna can be presented as,

$$G = eD \tag{14}$$

where D is directivity and e is the efficiency of the antenna.

An antenna's directivity is a function of its radiation pattern. It does not take into consideration the antenna's efficiency or input impedance. A practical antenna with a radiation efficiency less than 1 will not be able to emit its whole input power.

The equation shows that gain is proportional to the directivity [34],

$$G = eD = \frac{\text{Prad}}{\text{P(input)}} \frac{4\pi\ \text{Umax}}{\text{Prad}} \tag{15}$$

2.2.3 Polarization

Polarization characterizes the time-variation of the electric field vector of propagating plane wave. An electromagnetic wave consists of a magnetic field and an electric field. The tip of the electric field vector traces and ellipse in the plane orthogonal to the propagation direction, as illustrated in Fig. 10. If the ellipse is a circle, the polarization is circular, and if its aspect ratio becomes very large, it is called linear. In general, polarization is associated with two parameters: the axial ratio and handedness. The axial ratio is defined as the ratio of the larger semi-axis of the ellipse to the smaller. It takes very large values for linear polarization and equals one in the case of circular polarization. The polarization's handedness is defined as right-hand when the electric field vector rotates clockwise and left-hand when it rotates clockwise over time when the wave is moving away from the observer. The polarization of an antenna is defined as the polarization of the wave it transmits. [25]

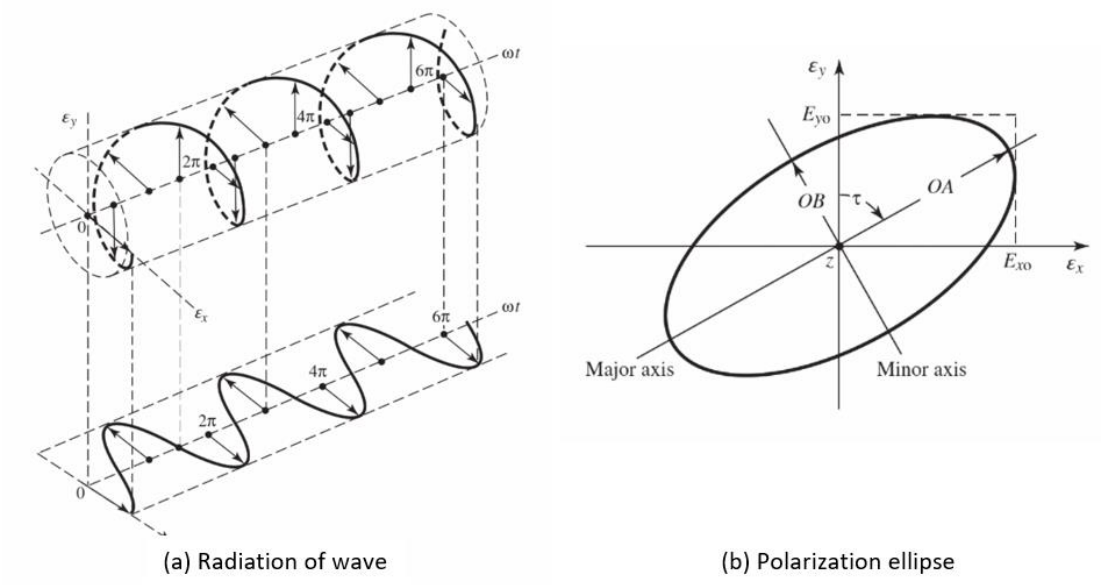

Figure 10. *Changing the direction of EM wave and polarization ellipse [25].*

Polarization of Antenna

In practice, it is very important to consider how the radio waves are polarized between transmitting and receiving antennas. As the transmitting antenna and receiving antenna reciprocate each other, the polarization must be similar. Otherwise, there will be polarization mismatch which is determined by Polarization Loss Factor (PLF). The polarization loss factor (PLF) refers to the amount of EM power that is lost due to polarization mismatch. If there is no polarization mismatch, it indicates that the antenna gets the maximum feasible power to capture the signal coming from the transmitter. It is noteworthy that polarization loss is unrelated to dissipation, but it is instead the antenna's inability to gather as much energy as possible from the incident wave [36,38].

Antennas are chosen depending on the application and the required length. Linear antennas, in general, provide a narrow but longer tag read field. Circular antennas provide a much broader but shorter tag read field. Circular antennas are used in the majority of applications, whereas linear antennas are used to read tags in specific areas. One of the features of circular vs. linear is that a circularly polarized antenna is harder to design and is typically a larger and more complex structure than a linear antenna. Therefore, the RFID tags are linear.

2.2.4 Read range

The read range of the tag is one of the essential factors that describe the performance of the tag antenna. The read range of a tag is the maximum distance at which the reader can read the information stored in the tag IC. In other words, the tag is hidden if the

distance between the reader and the tag is greater than the read range. The reason for this is either the antenna does not receive enough power to turn on the IC, or the backscattered signal strength at the reader is insufficient for detection.

The received power of an antenna can be defined by the Friis transmission formula [31],

$$P_t = P_t G_t G_r \left(\frac{\lambda}{4\pi d}\right)^2, \tag{16}$$

where, P_r is the received power by the receiving antenna, P_t is power of transmitting antenna, G_t and G_r are gain of transmitting and receiving antenna and λ is the wavelength, And d is the distance between the antennas.

If P_{th} is the equivalent transmission threshold power calculated under the perfect circumstances of free space, then the read range of an antenna can be derived from Friis' formula as following,

$$r = \frac{\lambda}{4\pi}\sqrt{\frac{\mathrm{Pt}}{\mathrm{Pth}}\tau GtGr} \tag{17) [31]}$$

The equation (17) is considering the polarization of the antennas are fully matched and there is no PLF considered. If the polarization mismatch is considered as a function of ($\boldsymbol{\Phi}$, $\boldsymbol{\theta}$), then is can be expressed as,

$$r = \frac{\lambda}{4\pi}\sqrt{\frac{\mathrm{Pt}}{\mathrm{Pth}}\tau Gt(\Phi,\Theta)Gr(\Phi,\Theta)p} \tag{18) [39][40]}$$

where p is the polarization coefficient [47]. The amount of radiated power by the antenna in a certain direction (EIRP - Effective Isotropic Radiated Power) can also be calculated from the read range equation. The transmission power P_t, and gain G_t is the transmission EIRP [39]. So equation (17) can be written as,

$$r = \frac{\lambda}{4\pi}\sqrt{\frac{\mathrm{EIRP}}{\mathrm{Pth}}\tau Gr} \tag{19}$$

Therefore, read range is also a function of EIRP of the transmitting antenna.[40]

2.3 Injection molding

Injection molding is making molded goods by injecting molten plastic material into a mold and then cooling it and hardening it. This technology is suitable for the mass production of goods with complex shapes and is widely used in plastic processing. Nowadays, injection molding is becoming more popular in creating packaging, automotive parts and components, toys etc. Injection molding is the process of injecting a polymer under high pressure into a mold and shaping it. The various steps in this procedure are relatively

brief. The entire injection molding process usually takes between 2 seconds and 2 minutes [41]. As indicated below, the injection molding process is separated into four key phases.

1. **Clamping**: Both parts of the mold must be closed before the material is pumped into it. A clamping unit secures them. After that, both sides are joined to an injection molding machine, and one-half can slide. The material is then injected while the clamping device presses the halves together, and both parts are securely held together as the material is injected. Larger machines (those with higher clamping power) require more time to shut and clamp the mold.
2. **Injection:** Plastic pellets are supplied into the injection molding equipment through a hopper. The injection mechanism propels these pellets toward the mold. The heat and pressure in the barrel serve to melt the pellets. The volume of substance injected is referred to as the 'shot.' This injection period is completed when the mold is filled to 95-99 percent of its capacity.
3. **Cooling:** The cooling process begins when the mold is filled up with melted plastic. When the plastic solidifies and cools, it will adopt the appropriate shape. During cooling, the component may shrink somewhat. The mold may only be opened when the cooling period has passed.
4. **Ejection:** The final stage is machine ejection. This is accomplished by the use of an ejection mechanism. When the mold is opened, the component is forced out with force because the part shrinks and clings to the mold. After ejection, the mold can be closed again, and another shot injected to restart the process.

The advantages of injection molding include cost-effectiveness, high output rates, and low wastage. One of the reasons plastic injection molding is so popular is that it is one of the more cost-effective methods of producing bespoke plastic components. Individual products may be produced rapidly and in large quantities due to the minimal cooling time (a few seconds) required between injecting the polymer into the mold and releasing the component. Furthermore, co-injection molding allows for the creation and production of several pieces at the same time. As it is simple to recycle any leftover or scrap molding plastic for future use, there is little waste in plastic injection molding.

However, injection molding has some shortcomings, such as high start-up costs to create quality parts that can ensure the efficient operation of injection molding. The parts or devices involved in this process are quite expensive as well as those parts have a high maintenance cost.

The in-mold labelled RFID tag is becoming very popular in the packaging market. RFID tags on IML products are demanding to the market distributors as individual identification of the products makes it very easy to track the item during buying-selling and shipment. As modern researches have overcome the limitation of RFID tag on IML products containing liquid and metals, level tagging is becoming more appealing and will improve the product's worth [6].

Injection molding is a method that uses a spinning screw and an external heating source to melt the granular or powdered material and then inject it into a mold to produce the matching product when the mold cools. It is a strong molding process capable of producing plastic objects in different shapes. A variety of plastic products can be manufactured by injection molding. Injection molding techniques may be applied to a wide range of materials, including plastic, polymers, and rubber, among others. Injection molding may also be done in various ways, including gas-assisted molding, water-assisted molding, micro-injection molding, injection foam molding, low-pressure molding, injection compression molding, and so on [41].

As mentioned before, injection molding happens in several steps; stage 1 is filling the materials inside the machine, in step 2, the melted liquid fills the chamber of the screw, and the last is holding. The screw pushes the melted material forward at a constant speed during the plasticizing step of the injection process. The material is compressed and continually transported onto the injection point. The pointer of the screw accumulates constantly and holds the liquid material until the command to inject. When the injection begins, the screw approaches ahead with increasing pressure on the material inside the mold until it gets filled. When the mold is filled up with the liquid, the temperature of the material continues to fall, so does the pressure in the mold cavity. Then the mold gets open, and the product comes out in the shape of the mold [42 - 44].

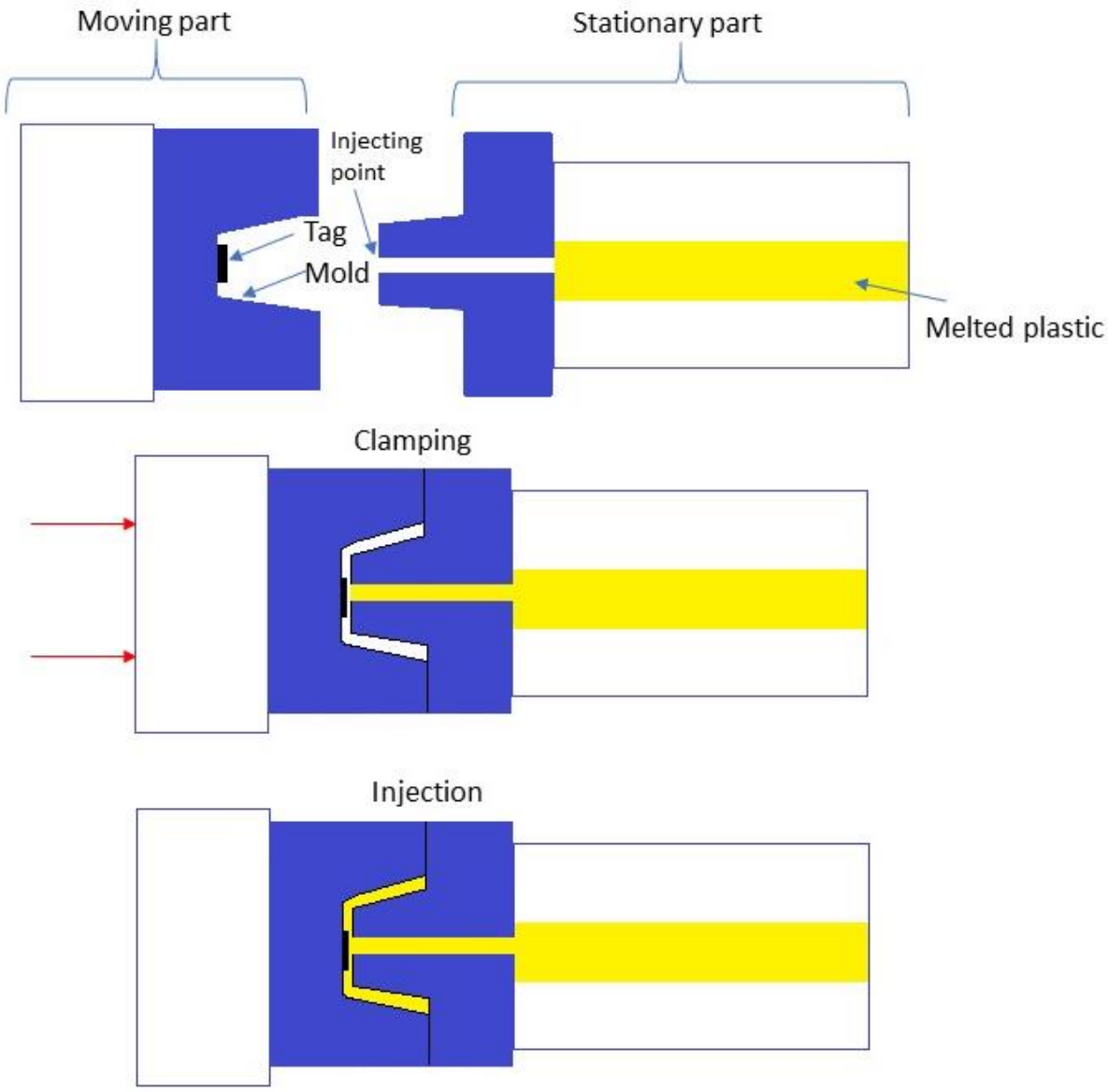

Figure 11. *In-mold mechanism*

As figure 11 demonstrates, the machine has two parts for molding; static and moving parts. For in-mold RFID products, the tag is placed in the moving wall in a certain position so that it gets labeled on the correct position of the product. The injection speed of a melted plastic must be extremely rapid (for example, 100 mm/s). Otherwise, if the melted plastic enters the mold slowly, it will cool down faster before achieving the desired shape, and molding will end up unfinished [32]. The width of the product and temperature distribution of the melted plastic on it are other crucial parameters of IML. The temperature of the liquid material becomes very crucial then, the product is supposed to have a thin wall, and the mold cavity has less space to hold the liquid. The lesser amount of molten plastic entering the mold cools quickly due to the colder walls of the mold. On the other hand, if the mold is wide enough, then it slows down the cooling rate of the melted plastic.

A large volume of hot liquid inside the mold will keep the heat for longer [18 -19]. There are other important parameters of this process, such as pressure, the flow rate of the liquid, the temperature of the mold, duration of the injection, and ejecting the product.

3. METHODS

It is mentioned previously that two Avery Dennison antenna designs are utilized in this experiment. Based on these designs, several prototypes are built on different substrates. The antennas are denoted as antenna 1 and antenna 2, respectively. The reason to select these two designs is their size dimension. Due to the size limitation of the IML machines from Tampere University, the tested antenna should have a length less than 70 mm and a width less than 10 mm. The dimension of the substrate is 73 mm in length and width of 13 mm. Figures (12) and (13) show the layout of the antennas and their geometrical dimensions. The two antennas have different IC bonding techniques; antenna 1 is for direct IC attachment, whereas antenna 2 is designed for strap IC attachment (mentioned in 2.1.3)

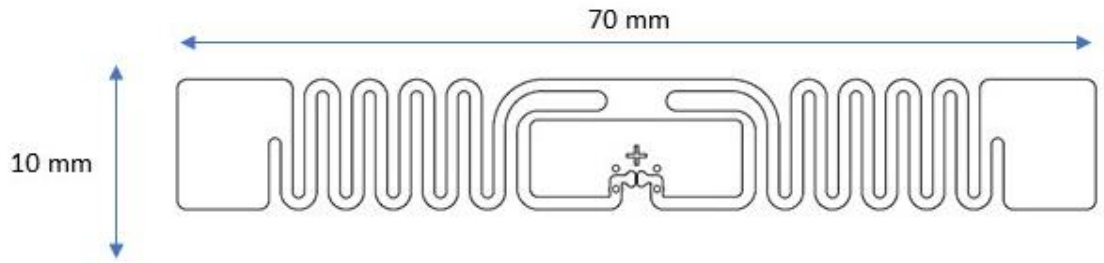

***Figure 12**. Antenna design 1 for direct-attached IC*.

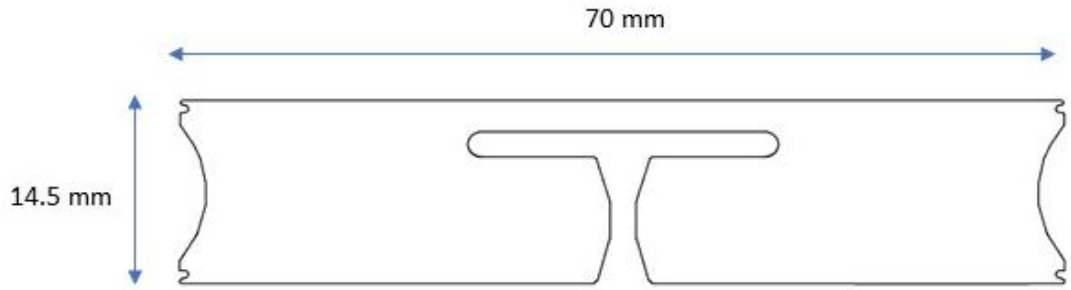

***Figure 13.** Antenna design 2 for strap attached IC*.

The experiment is executed in several steps, and analysis is done sequentially. The first step was to simulate the nominal designs to determine how to modify them by removing some areas as much as possible. After these modifications, the antenna designs were simulated again, and then the results were compared with measurement results. This chapter describes every step of executing the experiment.

3.1 CAD Tools

The design modification part is done with AutoCAD software. As mentioned before, for the IML trials, two Avery Dennison dipole antenna designs are implemented. To reduce the amount of metal or conductive ink from the antennas, the initial idea was to modify the nominal designs by removing some parts from the different areas of the antenna. Before the modification, the nominal designs were simulated in HFSS to observe the current distribution of the antenna. Before any modification, it was essential to study which regions of the antenna are actively radiating so that the most active parts would remain intact and other areas could be modified. According to HFSS simulation results of the nominal designs, it is noticeable that the middle part of the antenna near the IC pad area has the highest current density. This phenomenon is applicable for both selected antennas. Therefore, the modification should avoid these areas. To reduce the amount of metal or ink from the antennas, mesh patterns shown in figure (14) have been used to replace the selected areas but still maintain the symmetrical structure of the design.

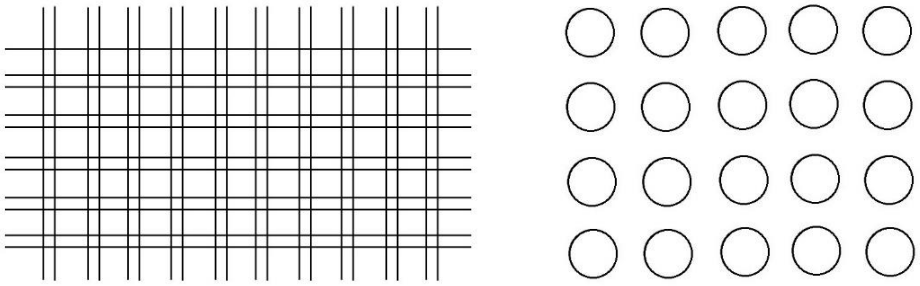

(a) (b)

Figure 14. *Examples of different mesh patterns; (a) square mesh (b) circular mesh*

According to the simulation results, the selected modification area was the end of the dipoles. As the edges are also significant to keep for the current flow of the antenna, around 2mm border would remain uncut. It is observed that if the border is less the performance of the antenna starts to degrade. The following figure 15 shows the areas of the antenna that significantly contribute to its radiation from the simulations. The current density in the figures is in normalized form. The red areas have the highest current density, and it reduces gradually with green and then blue regions.

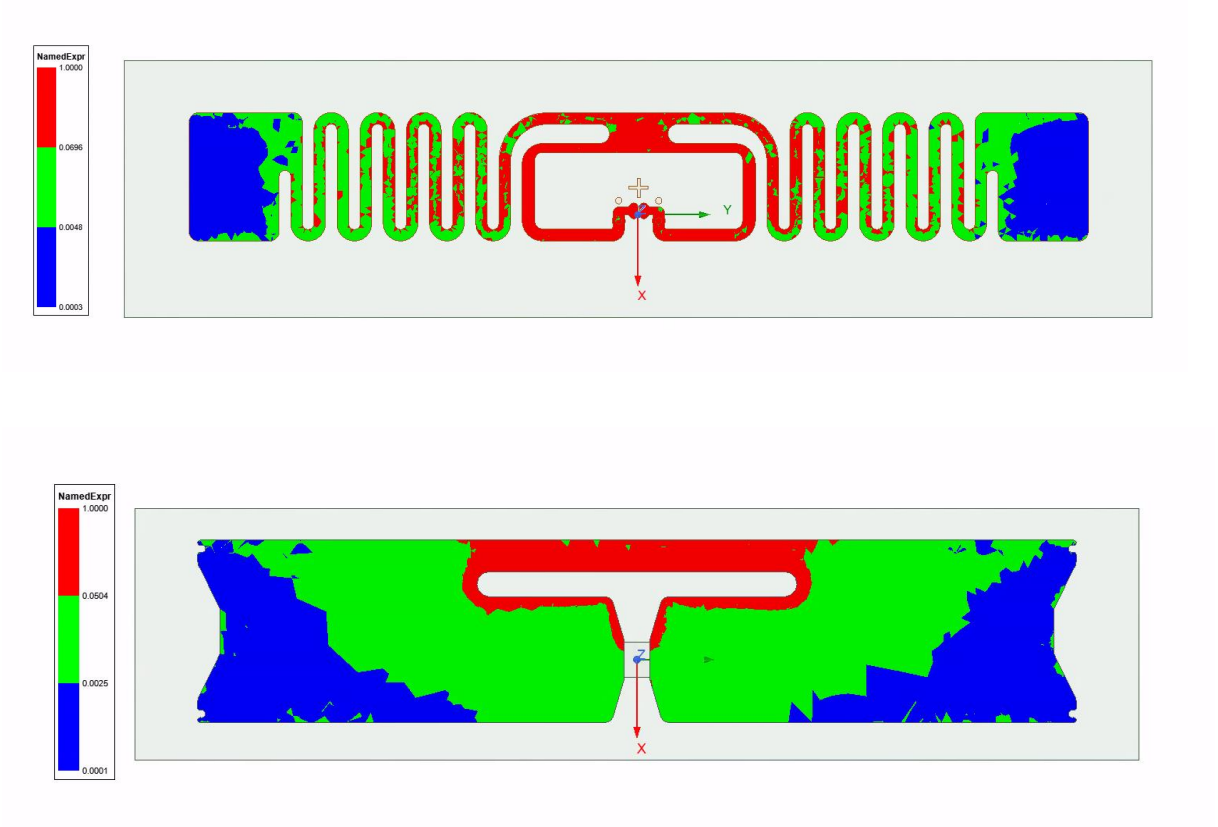

Figure 15. *Actively radiated areas of the antennas*

Figure (16) shows the selected areas to remove metal or ink from the antenna. The dotted lines illustrate the removable regions of the antenna.

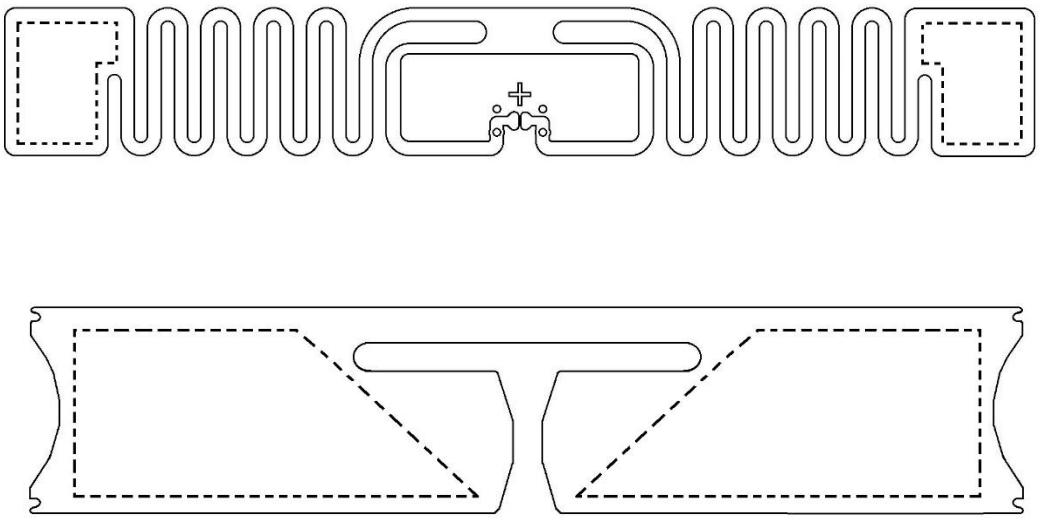

Figure 16*. Selected areas to remove metal or ink from the antenna.*

After modifying the antenna designs, both variants (nominal and modified) were tested in an anechoic chamber. The read range of the variant antennas was almost identical. The performance of the modified design starts to degrade if the edge is thinner than 2mm (more details in the result section). Therefore, in the selected variants, the edge is kept to be 2 mm. The material of the antenna in simulation and is aluminum on Polyethylene Terephthalate (PET) substrate. Table 1 shows the properties of the material considered in HFSS simulation.

Table 1. *Material properties of HFSS simulation.*

Materials	Relative permittivity (F/m)	Di-electric loss tangent	Relative per-meability (H/m)	Bulk conductivity (s/m)
Aluminum	1	0	1	$38x10^6$
PET	3.07	0.023	1	0

Figure 17 (a) and (b) shows all the variants of the nominal designs along with the mesh patterns.

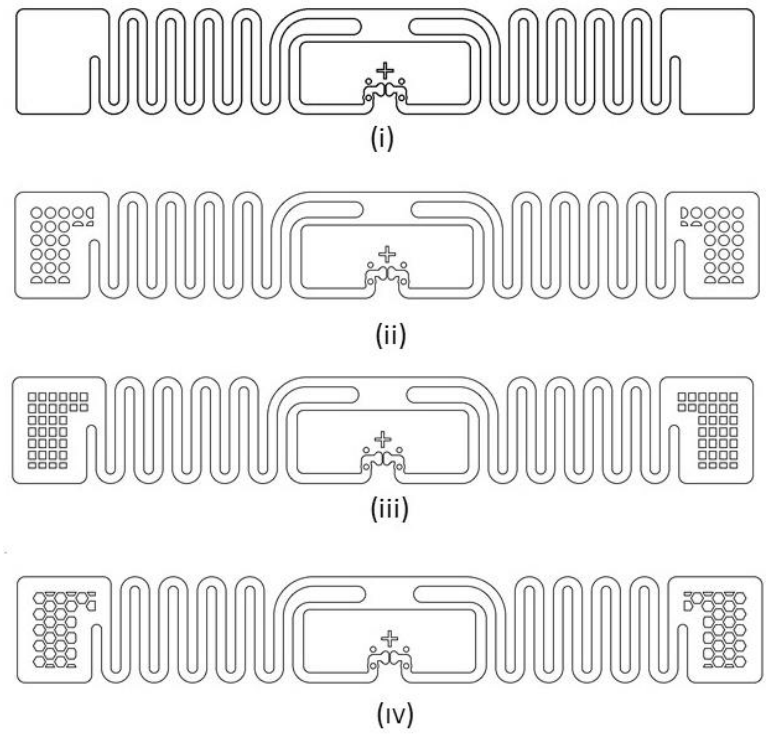

(a)

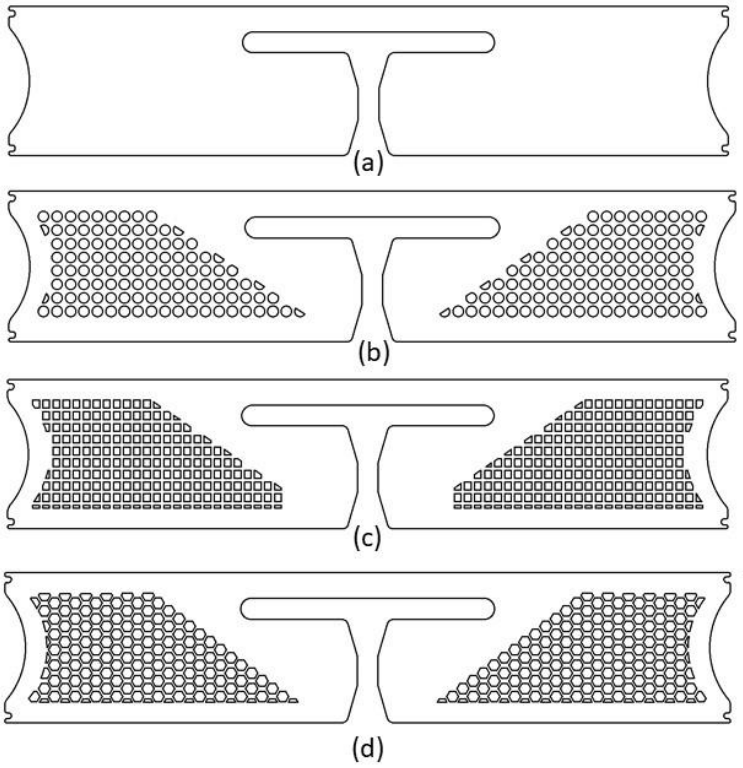

(b)

Figure 17*. variants of the nominal designs along with the mesh patterns; (a) antenna 1 (i) with (ii) circled mesh (iii) square mesh (iii) honeycomb mesh, antenna 2 (a) with (b) circled mesh (c) square mesh (d) honeycomb mesh.*

3.2 Electromagnetic Field Simulation

A full-wave electromagnetic simulator predicts the electromagnetic field response of a defined structure corresponding to a given excitation source(s), such as a voltage source or an incident plane wave, within a given physical domain. Typically, they also predict how the electromagnetic energy radiates out from the domain and distributes to the surrounding space far away from it. ANSYS HFSS used in this work is commercial full-wave EM simulation software that considers 3D domains and is based on the finite element method (FEM).

During the simulation, the geometric area of the simulation object automatically gets divined into a large number of small tetrahedra elements. These elements are called mesh elements of simulation. The accuracy of the simulation depends on the quality of the mesh in the simulation. Choosing an accurate number for mesh is preferable so that the tetrahedra elements are fine enough to achieve an accurate field solution. On the other

hand, if the number of mesh elements (tetrahedral areas) is very small, the simulation speed becomes very slow [45]. The following figure 18 shows the mesh elements of antenna 1 during simulation.

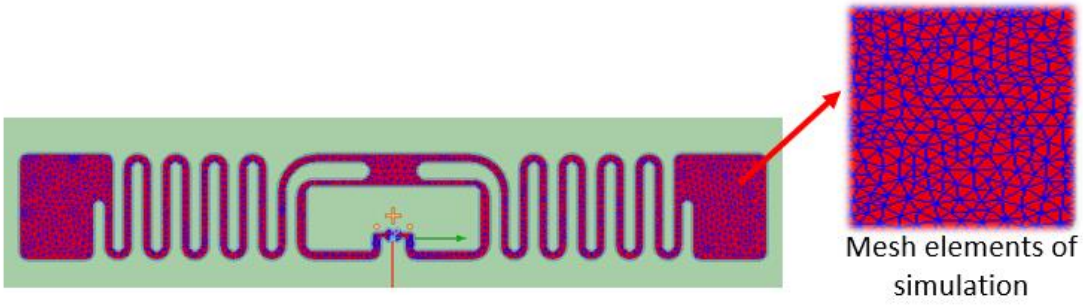

Figure 18. *Mesh elements of antenna 1*.

After finalizing the antenna modifications, all the variants have been simulated in Ansys HFSS software. It was to observe the fundamental parameters of the designed antennas. The focused parameters in these simulations are the read range, the antenna's resonance, and the power transmission coefficient. For each nominal design, three types of mesh patterned design have been simulated in HFSS. The simulations represent that the antenna's performance before any modification and after modification by removing partial areas is almost identical. The simulation frequency was considered from 800 to 1000 MHz. HFSS simulation results are discussed elaborately in section 4.2.1.

3.3 Thermal distribution analysis

Thermal distribution analysis refers to observing the temperature distribution on a solid surface. Ansys Icepak provides electronic temperature solutions that utilize the Ansys Fluent computational fluid dynamics (CFD) solver for thermal and fluid flow analyses. This simulation tool enhances design performance and eliminates the requirement for trailing hardware setup for uncertain results, which is very cost-effective.

Besides the antenna parameter analysis in HFSS, a heat simulation is executed in Ansys icepak. As it was assumed that the wrinkled antenna is the result of uneven heat distribution of the metallic parts of the antenna, it was essential to observe how heat is distributed on the surface of the antenna. As described in section 4.2.2, there are a lot of small details in the IML process to demonstrate in the simulation. To display all the practical details in a simulation environment could be way too complex. It was not possible to show the mechanical force of the melted plastic as well as the flow of liquid in the

icepak simulation. Therefore, a simple version of the IML process has been illustrated in the simulation of icepak.

In the practical case, the antenna is placed on the mold, and it moves to the static wall where liquid plastic of 220°C fills the mold from one specific point and spreads it all over the antenna. In the simulation, the antenna has been placed on a metallic plate, and two blocks have been placed on each side of it. The temperature of one block is considered as 220°C (according to the real temperature of the melted plastic) and another block of 40°C (temperature of the mold). The main goal of the heat simulation is to see which part of the antenna gets heated first and the most. Theoretically, when one block is hotter than the other block, the heat transition should be uniformly distributed, and the antenna should be heated evenly all over the areas. In reality, the liquid does not touch the whole antenna at the same time. As the liquid starts to spread from one point and spreads all over; therefore, there should be some temperature shock in the antenna surface even though the molding happens very rapidly. This detailed scenario is not possible to show in the simulation environment. Therefore, a simple steady-state simulation environment has been presented.

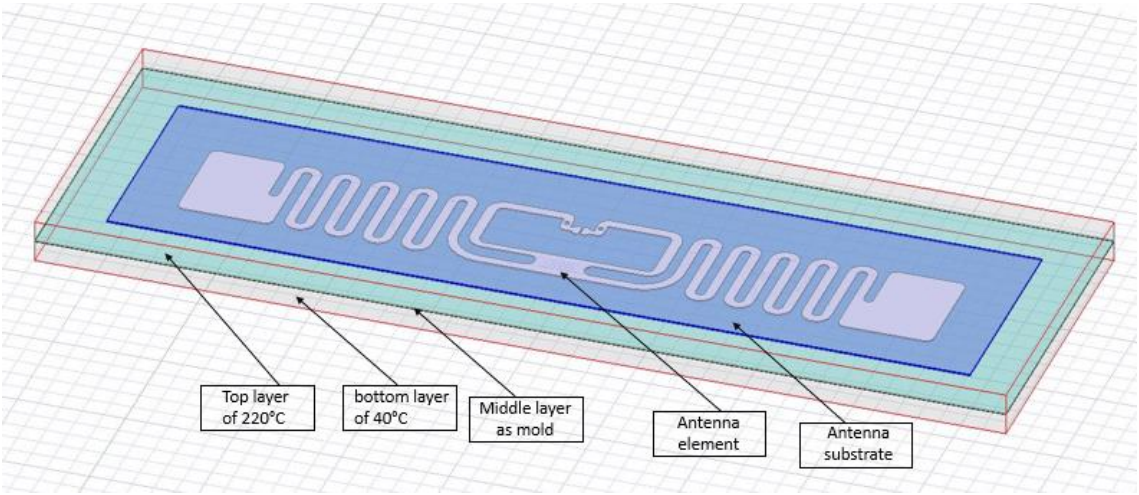

***Figure 19**. simple representation of IML in heat simulation*.

3.4 Screen Printing

Screen printing is a simple and widely used method for producing flexible printed antennas. During this procedure, a plastic frame known as a screen is created with certain gaps in the shape of the antenna. The screen is then loaded into the screen-printing machine. The machine has a flat blade that swipes over the screen. The required conductive ink is then put over the screen, and the flat blade swiping back and forth drives the ink on the screen. Because the screen has gaps or holes, the ink falls through the

gaps and lands on a substrate positioned beneath the screen. This is how printed antennas are created via screen printing on various substrates [46]. The process is illustrated in figure (20).

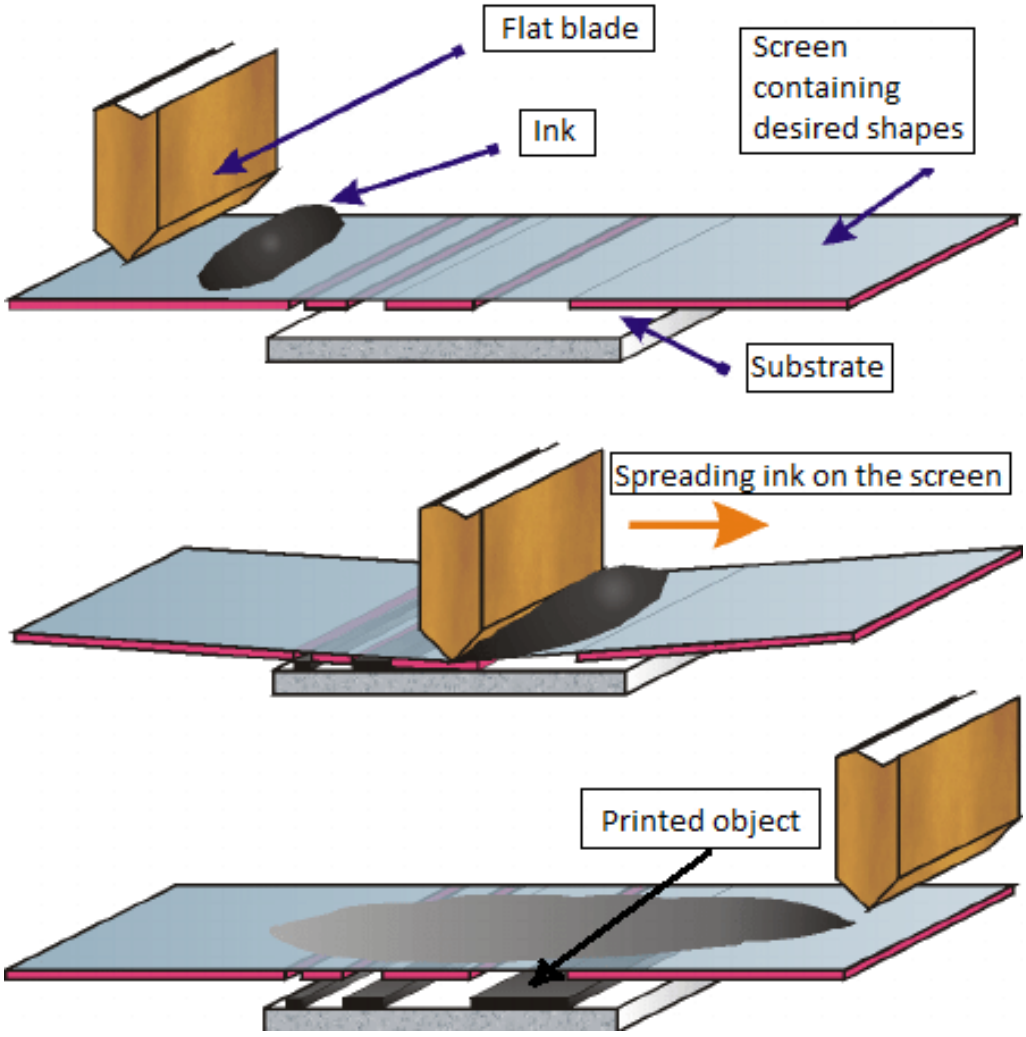

Figure 20. *Screen printing [47]*

For the IML trials, besides the metal samples also some conductive ink printed antennas were planned to examine. Some variations were prepared in different stretchable conductive inks by using the screen-printing method. The following figure shows the screen designed for the antennas and, after printing, how it looks.

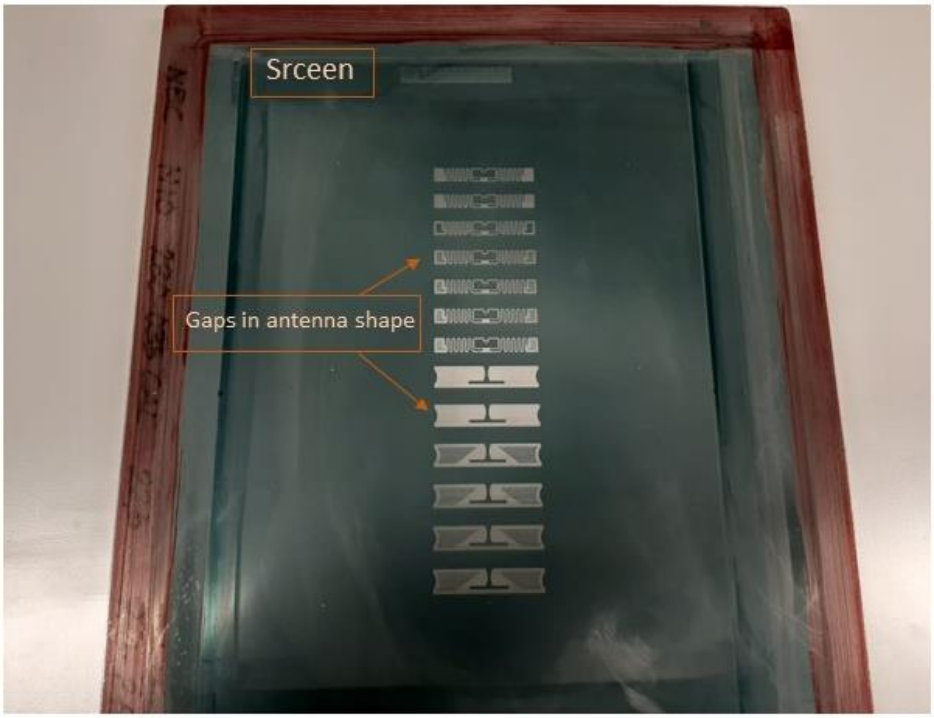

Figure 21. *Screen for printing*

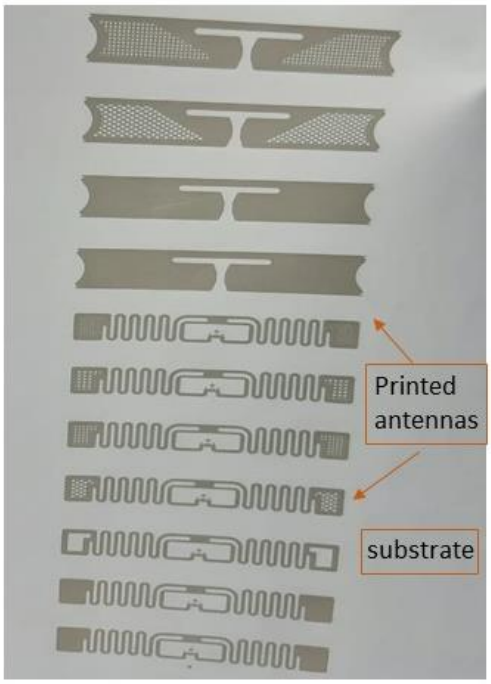

Figure 22. *Printed antennas after screen printing*.

3.5 Injection molding with RFID tags

As the main goal of this study is to test the antennas in the IML process. The final step of the analysis was observing the antennas after injecting plastic into it. For the IML trials, about 100 laser cut metallic antennas, and screen-printed antennas on different substrates have been examined at Tampere University. As shown in figure 23, the desired RFID tags consist of 4 layers (with strap) or 3 layers (direct IC); adhesive, antenna, IC strap (some antennas had directly attached ICs), and the cover or face material to disguise the antenna shape. The tag was placed on the moving part of the IML machine with adhesive and different kinds of plastic polymers were used as the melted liquid. During IML tests, it is very important to optimize the temperature of both mold and plastic liquid, the flow rate of the liquid, and the pressure or force of injecting liquid inside the mold to get the desired molded product in optimum shape. For this case, the mold temperature was kept around 40°C, and the melted plastic was 220°C.The flow rate of the liquid was 100 mm/s, and the maximum pressure inside the screw chamber was 388 bars. Though two separate trials have been done at the university with different antenna substrates and plastic materials, yet the results were quite similar (detail discussion in section 4.3).

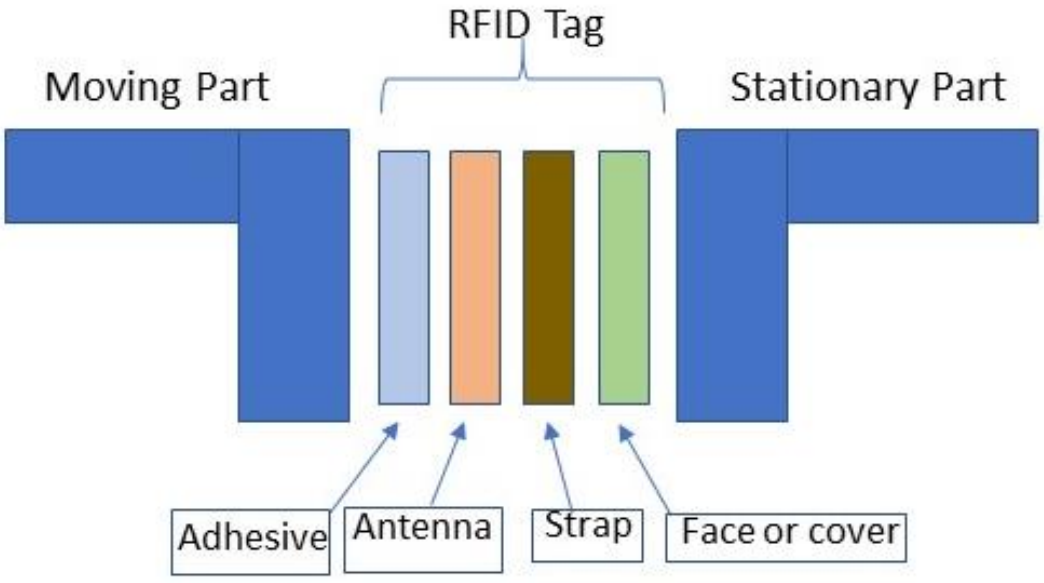

Figure 23. *Antenna layers for IML*

The purpose of using the adhesive layer of the IML samples was to stick the RFID tag with the mold (moving part) in a specific position. The adhesive layer is very important to

use; otherwise, the tag does not stay in the correct position and gets displaced after the process (shows figure 24). A thin layer of adhesive was used to get rid of this problem.

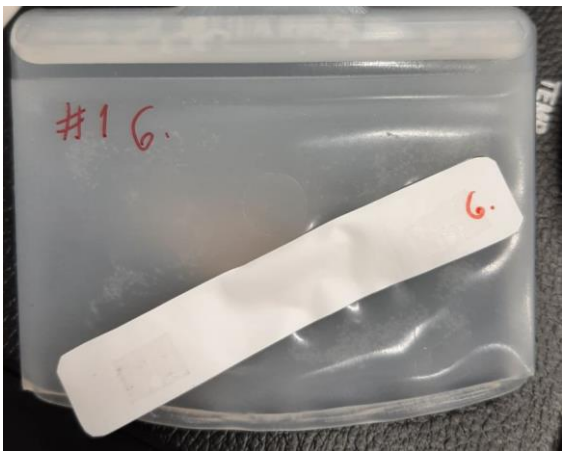

Figure 24. *Displaced sample without adhesive layer*.

3.6 RFID tag characterization

After the IML trials, it was important to investigate how the in-mold samples performed in terms of the parameters considered for simulation and tagformance measurements. It was also a matter of concern whether the strap attached or direct-attached ICs survived after the heat and pressure from the IML process. It was expected that the performance of the in-mold samples will not be the same as the inlays before IML, as the permittivity and thickness of the plastic will affect the resonance frequency of the antennas. As mentioned before, all the variants have been measured in anechoic chambers and the performance of the antennas has been analyzed with Voyantic Tagformance UHF tools [36]. It has been found that both categories of ICs survived the IML process, and the tags were functioning well. Even Though there were some wrinkles on the face material (reasons described in the result section 4.3).

Voyantic Tagformance is a very high-tech tool to measure the far-field and near-field characteristics of RFID tags. The Tagformance tools are connected with an anechoic chamber. In RFID communication, the reader sends a modulated signal to the tag to activate it, and the tag reflects the signal back to the reader. Tagformance measures the properties of the transponder while it is active. The Tagformance tool includes measurement software operated in a computer attached to the system. The waveforms to measure the characteristics of the tag such as read range, tag sensitivity, transmitted power shows via this software [49].

4. RESULTS AND DISCUSSION

4.1 Measurement and performance analysis of prototype antennas

The previous chapter mentioned that antenna prototypes of the nominal designs are chosen based on their performances, mainly based on the tag read range. In this section, the analysis of the antennas is described in more detail.

To compare the read range, both forward and reverse operations are considered. Figure 25 shows the read range of antenna 1 in its nominal design without any sections removed and the read range after removing the center parts of the dipoles while retaining 2mm and less 2 mm of the antenna's edge. It is noticeable that the read range of the nominal design and antenna with 2 mm edge is almost identical. Both antennas have the almost same read ranges with a maximum difference of 0.5 m in forward (figure 25(a)) and around 1m in reverse operation (figure 25(b)). The performance of the thinner-edged antenna degrades in both forward (maximum 1m) and reverse (maximum 5m) read range. The application requires the measurement bandwidth is from 800 MHz to 1GHz. Therefore, the read ranges are compared in this range.

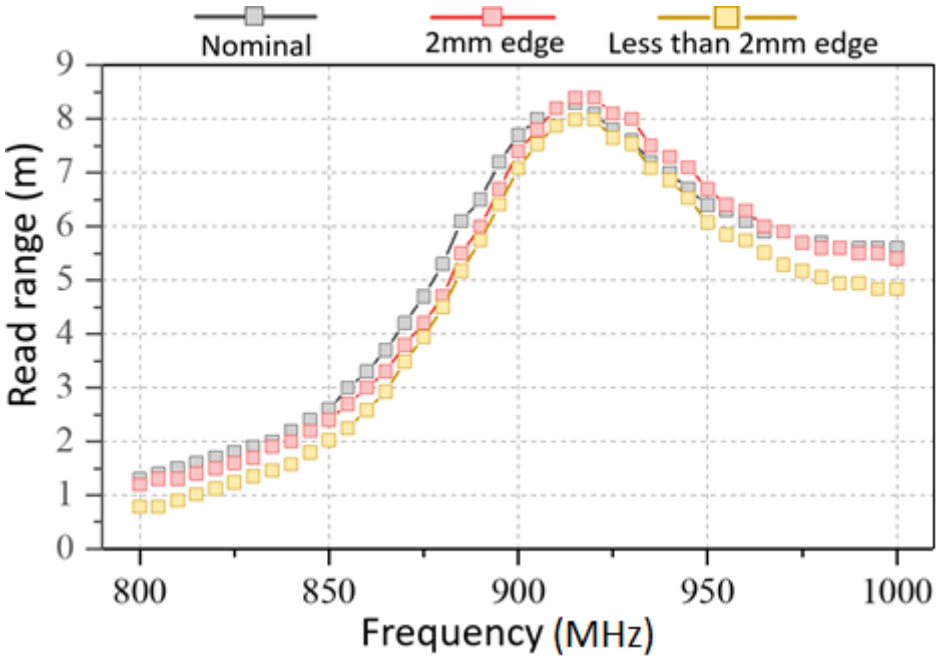

(a)

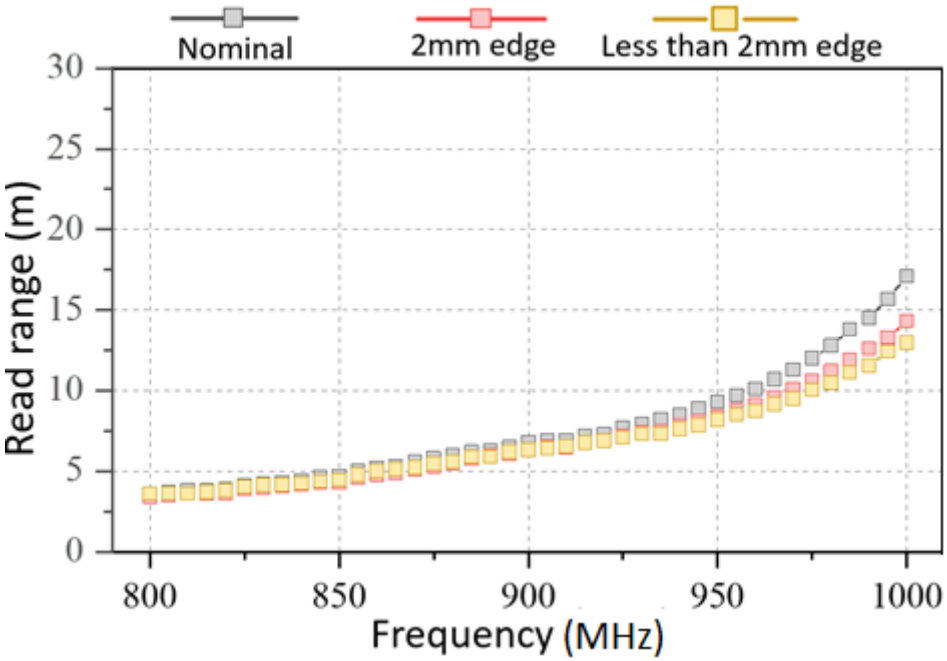

(b)

Figure 25. *Read range of antenna 1 without removing any areas, after removing some areas maintaining 2mm edge, and less than 2mm edge; (a) forward read range, (b) reverse read range*.

The same analysis is done for antenna 2 as well. The comparison of read range is quite significant in both forward and reverse operation that the thinner edged antenna has less read range than the other antennas (see in figure 26).

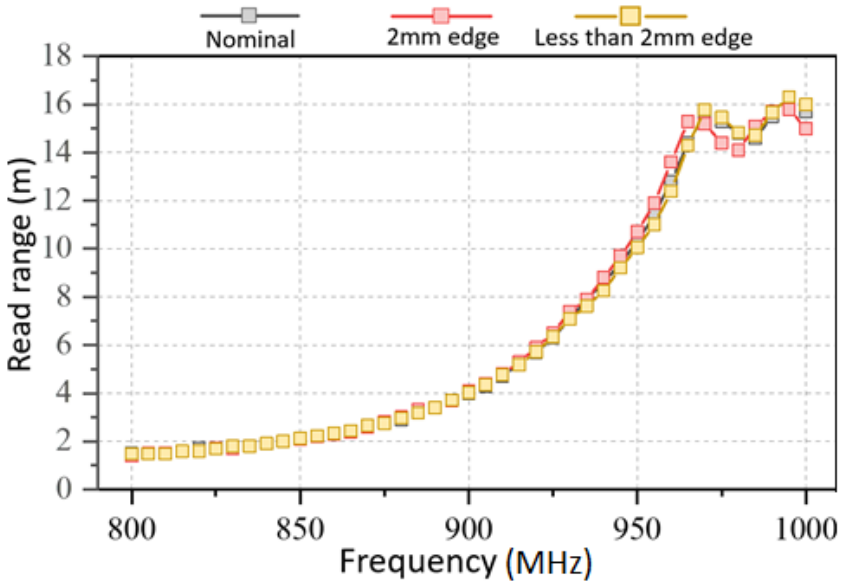

(a)

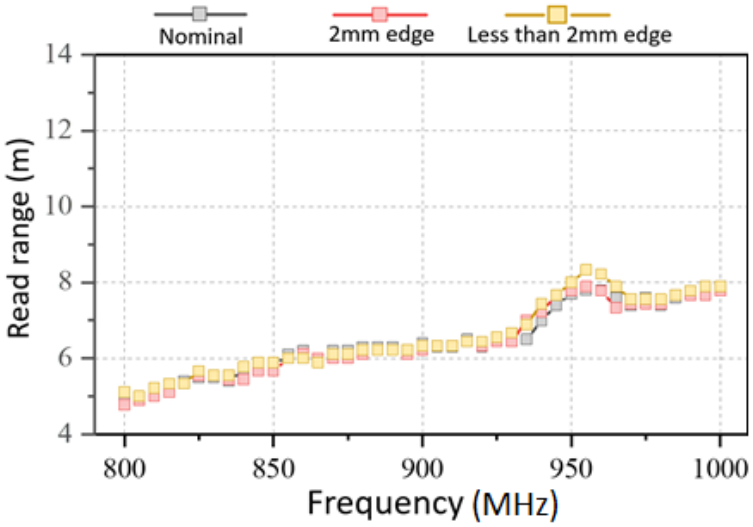

(b)

Figure 26. *Read range of antenna 2 without removing any areas, after removing some areas maintaining 2mm edge, and less than 2mm edge*.

Figure 26 shows that, the difference between the prototypes is very small and in fact, "less than 2 mm" seems to have the highest ranges for antenna 2.

From the analysis mentioned above, it seems that having 2 mm edge is sufficient to maintain the antenna properties when compared to the nominal case. Moreover, an even thinner edge could be ok, but that study can be left for future works.

For the IML trials, it was required to verify how the sample looks after injecting plastic if the selected areas of the antennas are removed completely or partially. To remove the areas partially, some geometrical mesh patterns (shown in figure 17) are applied in the dotted areas. Figure 27 and 28 illustrates how antennas 1 and 2 performs after applying mesh patterns on them. It is observed from the read range of the antennas that the variations with different mesh patterns behave likewise the uncut antenna.

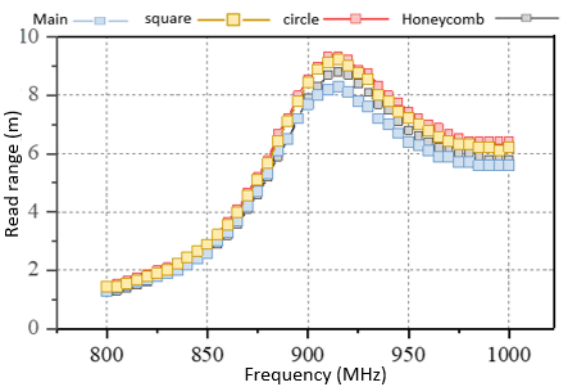

(a)

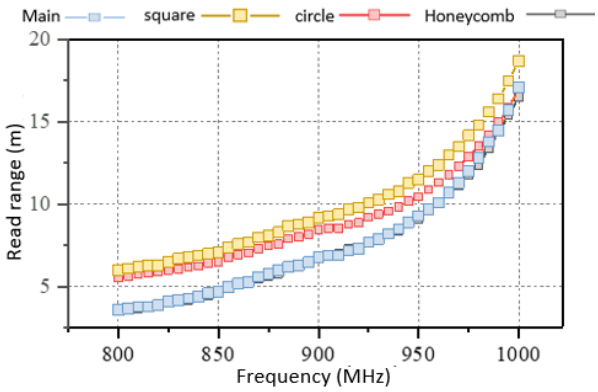

(b)

Figure 27. *comparing read range of unmodified antenna 1 with removing some areas by applying different mesh patterns*.

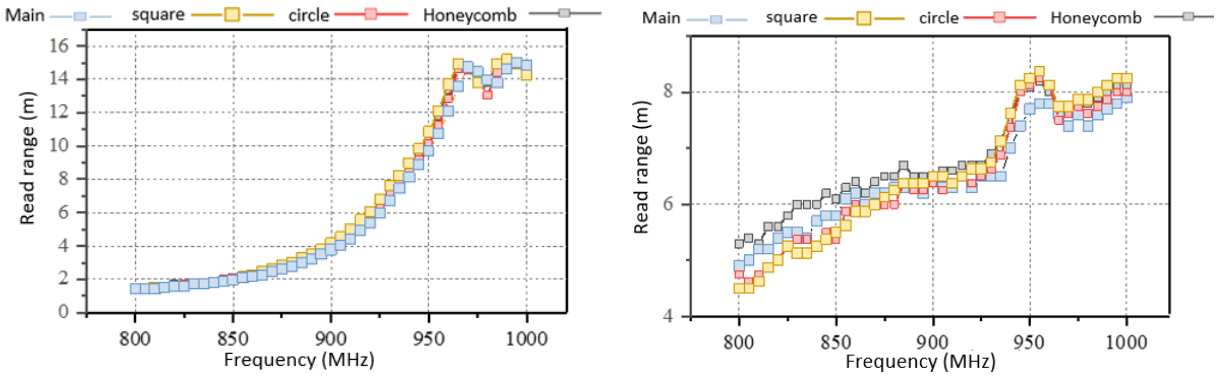

Figure 28. *Comparing read range of unmodified antenna 2 with removing some areas by applying different mesh patterns*.

In this section, it can be concluded that the performance of a meandered dipole or usual dipole antenna of a specific length can remain unchanged if areas with low current density get entirely or partially removed.

4.2 Simulation results

To analyze the antenna characteristics, two types of simulations are done using Ansys HFSS and Icepak. The general parameters such as antenna gain, impedance, read range, etc. are observed in HFSS. The motivation to simulate in icepak was to observe the heat distribution of the antenna elements. The analysis that is done through simulation is discussed in this section in detail.

4.2.1 EM field Simulation results

Simulation of the nominal designs

The nominal designs and all the variants are simulated in Ansys HFSS to compare their performances. The nominal designs are observed by their EM characteristics (e,g; gain directivity, efficiency, impedance matching (matching antenna impedance with IC impedance), power transmission coefficient and read range). The variants with mesh patterns are compared with the nominal design by their read ranges within 800-1000 MHz.

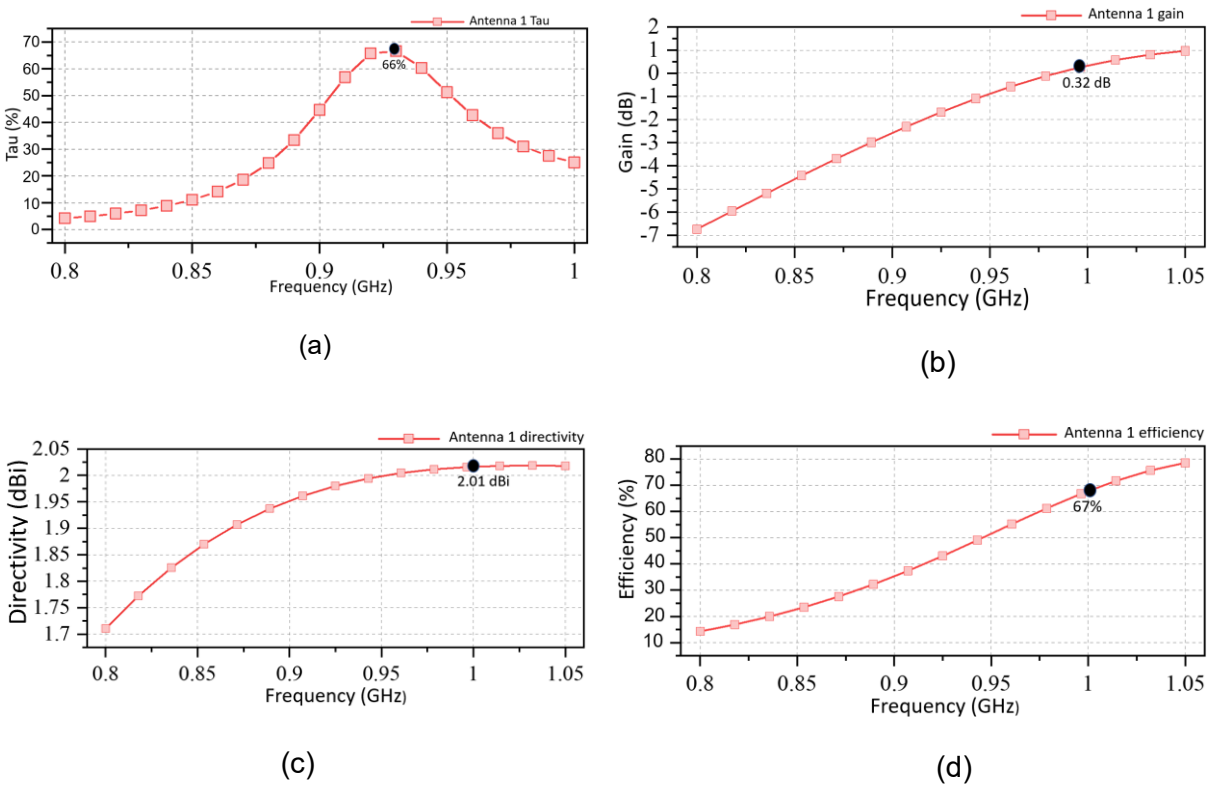

Figure 29. *EM characteristics of Antenna 1; (a) Power transmission coefficient (tau), (b) gain, (c) directivity, (d) efficiency*.

Figure 29 illustrates Some essential parameters of the nominal design of antenna 1. In figure 29 (a), the power transmission (τ) shows maximum power (66%) is transmitted at around 0.93 GHz. The maximum gain of the antenna is 1 dB at 1.05 GHz, but within 1 GHz, the maximum gain is 0.32 dB (in figure 29 b). The maximum directivity of the antenna is 2.01 dBi at 1 GHz with an efficiency of 67% (see figures 29 c and d).

Figure 30 shows the impedance matching between antenna 1 and the IC. Both reactance and resistance are plotted in 30 (a) and (b). It shows the similarity of the matching point and the resonance of the antenna. In the case of antenna 1, the IC resistance is 2060 Ω, and reactance is 0.953 pF.

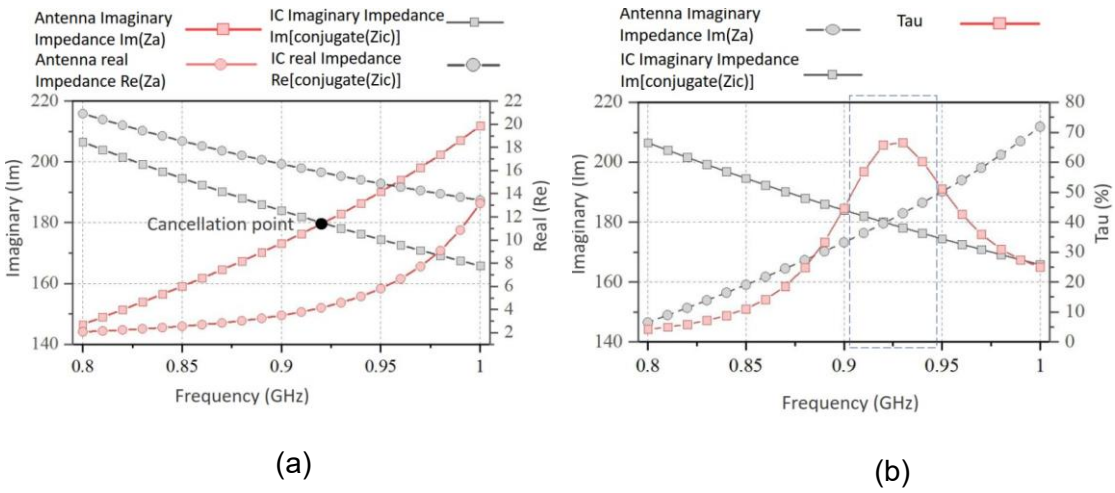

Figure 30. *For Antenna 1 (a) Complex conjugates of antenna and IC, (b) Power transmission coefficient (tau) with reactance cancellation point*.

Likewise, antenna 1, the EM characteristics of antenna 2 are shown in figure 31. The antenna's resonance is at 0.99 GHz with τ of 85% (figure 31 (a)). The maximum gain of the antenna is 1.25 dB, directivity of 1.54 dBi with an efficiency of 75% near to 1GHz (in figure 31 (b-d)).

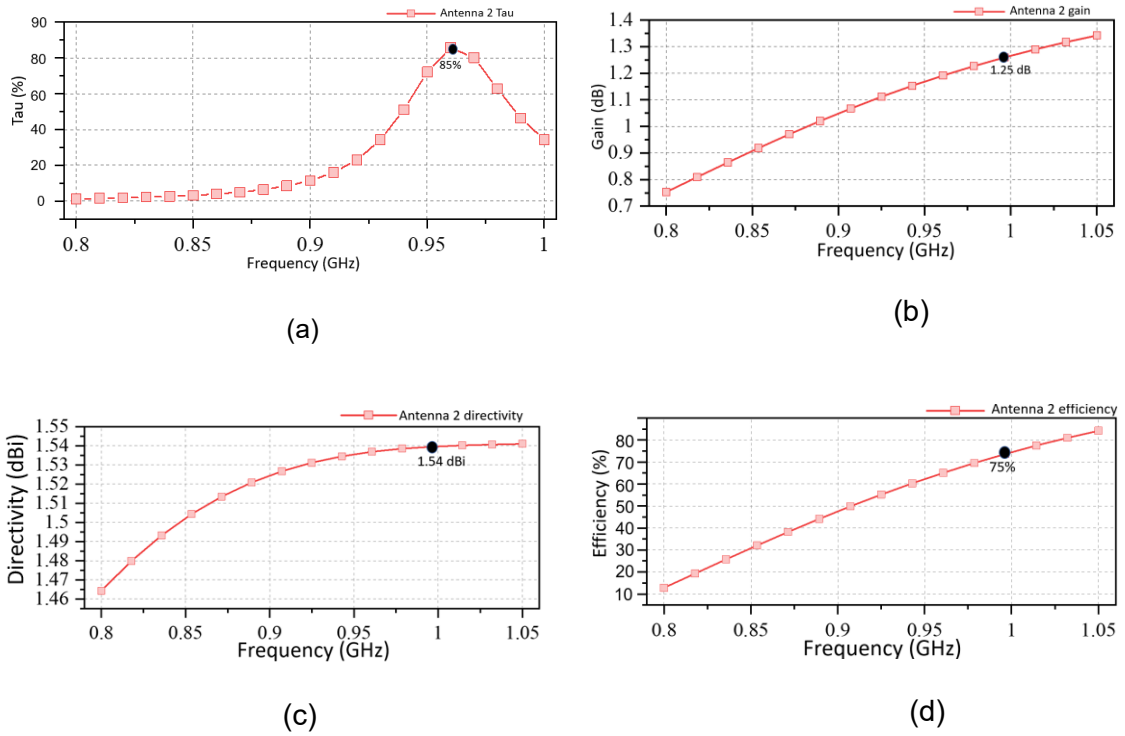

Figure 31. *EM characteristics of Antenna 2; (a) Power transmission coefficient (tau), (b) gain, (c) directivity, (d) efficiency*.

The impedance matching of antenna 2 is represented in figure 32(a). The resonance frequency matches the reactance cancellation point in figure 32 (b). In case of antenna 2, the IC resistance is 2790 Ω and reactance is 0.905 pF.

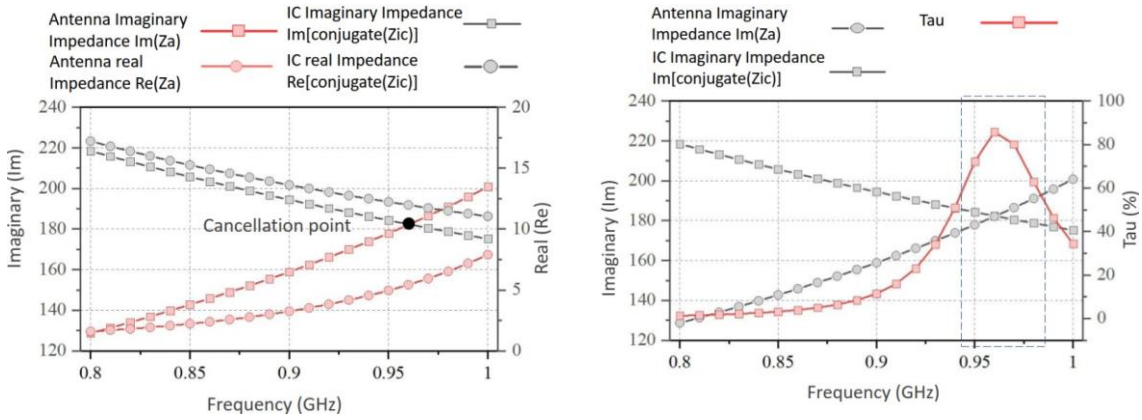

(a) (b)

Figure 32. *For Antenna 2 (a) Complex conjugates of antenna and IC, (b) Power transmission coefficient (tau) with reactance cancellation point*.

Based on the analysis above, antenna 2 has better performance compared to antenna 1. The gain, directivity, and efficiency are higher of antenna 2. If the antenna design would affect IML tags, then antenna 2 would be preferred in terms of performance.

Comparing nominal designs with mesh patterned variants:

All the variants of antenna 1 and antenna 2 with different mesh patterns (in shape of circle, square and honeycomb) are simulated in HFSS. To maintain concise presentation, the antennas are compared in terms of their read ranges only. The simulated read ranges are the forward read ranges of the antennas. Therefore, the forward read range from the measurement results (from section 4.1) is compared with the simulated results. Figure 33 (a) shows the read ranges achieved from simulation, and figure 33 (b) shows the read ranges from anechoic chamber measurement using Voyantic Tagformance UHF tools.

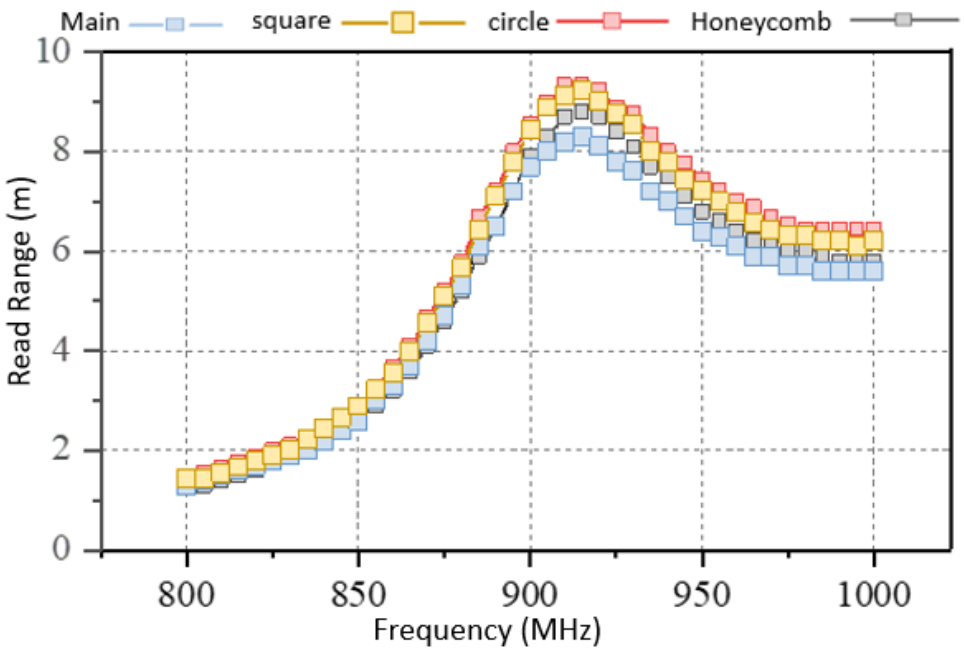

(a)

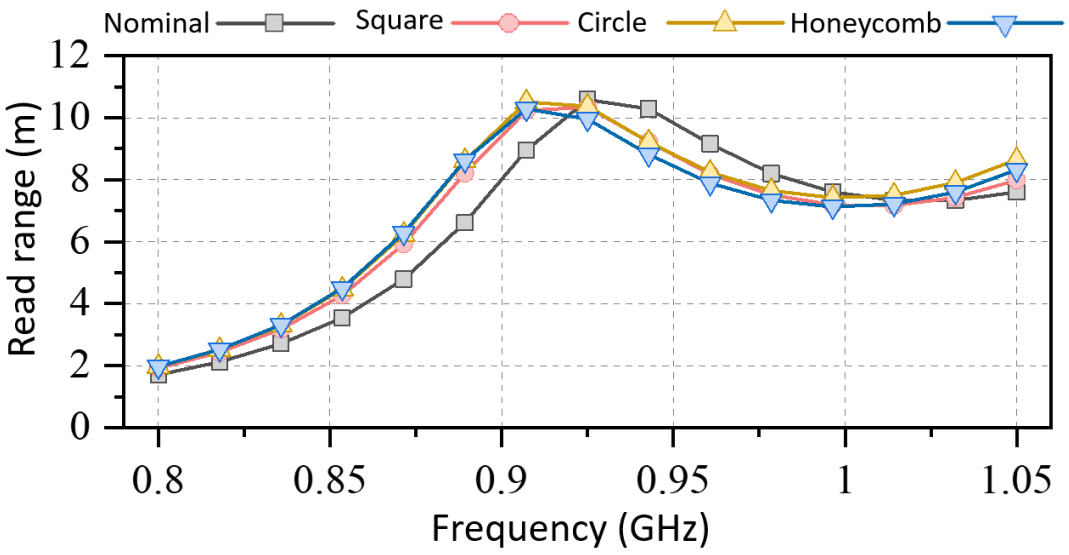

(b)

Figure 33. *Forward read ranges of antenna 1 nominal design and variants, (a) measurement results, (b) simulation results*.

The simulation results are slightly different than the measurement results. Firstly, the read ranges are higher in simulation (10.2 – 10.5 m). In practical measurement, the reduced read range (8.5 – 9 m) can be caused by the antenna placement or environment during measurement. Secondly, the resonance of the mesh pattern designs is slightly shifted towards the left (around 0.02 GHz). Even though the shift is minor, but still the reason for this is explainable. There are very tiny holes in the mesh designs, and the distance among them is around 0.2 to 0.5 mm. During simulation, managing these small

areas and defining the sufficiently dense computation mesh (small tetrahedra elements) without blowing up the simulation time and memory consumption is a crucial challenge. If the mesh or tetrahedra elements of the simulation is very fine for these small areas, the simulation time would be too long to execute (more than 15 minutes). Therefore, a moderate timing for the simulation is considered in comparatively less fine mesh elements (5-6 minutes). Thus, in the simulation results, the mesh patterns show slight variations in terms of frequency shifting.

Similar phenomena also happen in the case of antenna 2. Figure 34 (a) and (b) shows measurement and simulation results of antenna 2. In this case, the resonance of the variants is shifted toward the right (about 0.4 GHz) and slightly higher read range. The overall read ranges of simulation and measurement results in antenna 2 are very similar (around 16 m).

Though there are very few differences between the results, it is noticeable that the antenna variants perform very similarly to the nominal designs. Therefore, it can be concluded that if the less active areas of the antenna are removed, it can still perform the same with reduced amount of conductive ink or metal.

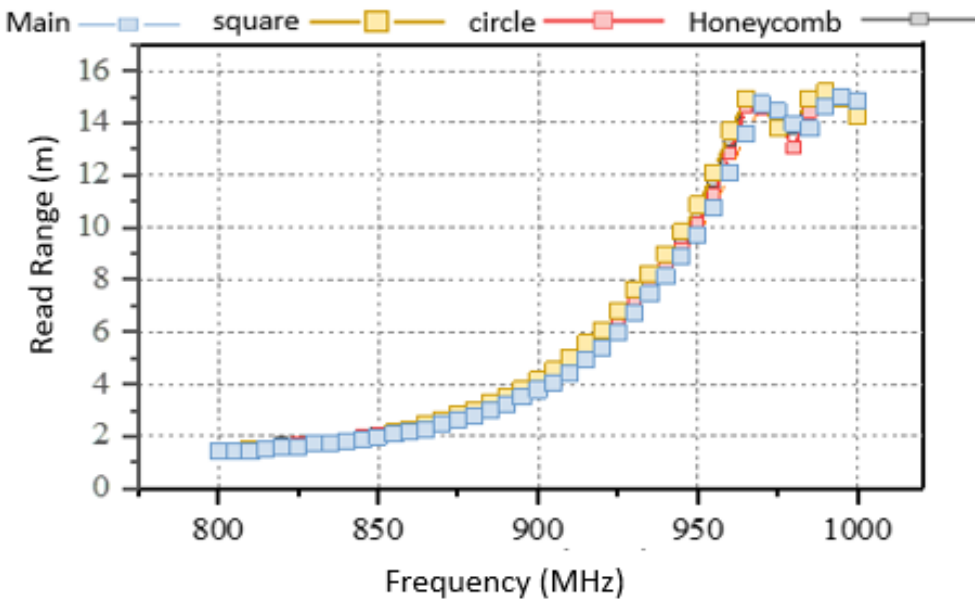

(a)

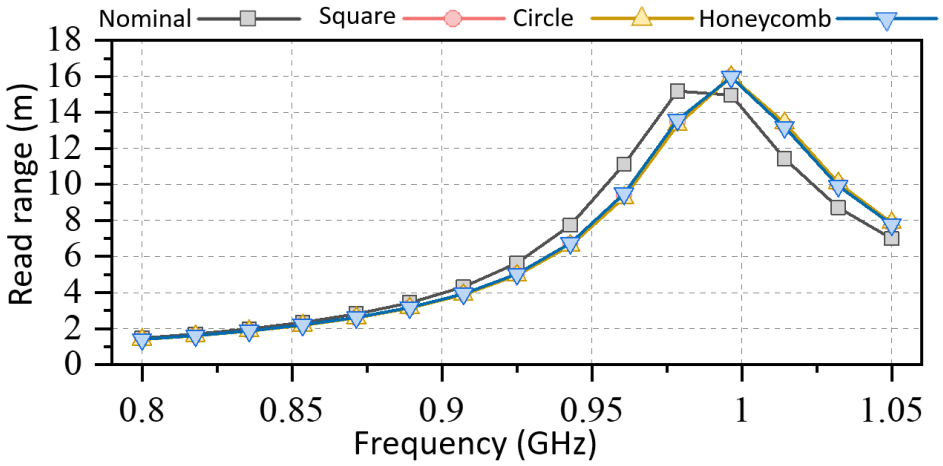

(b)

Figure 34. *Forward read ranges of antenna 2 nominal design and variants, (a) measurement results, (b) simulation results*.

4.2.2 Heat simulation results

The Heat simulation is done to imitate the IML process and observe how temperature distributes on antenna elements. As described in section 3.3, there are two walls in the IML process. The moving wall holds the antenna on the mold, and melted plastic goes into the mold coming from the stationary wall. The mechanical process is challenging to demonstrate in this kind of simulation; therefore, a simple version is implemented. Figure 35 shows how the simulation is done in a static approach. Static approach refers that, no liquid flow of melted plastic was presented in this approach.

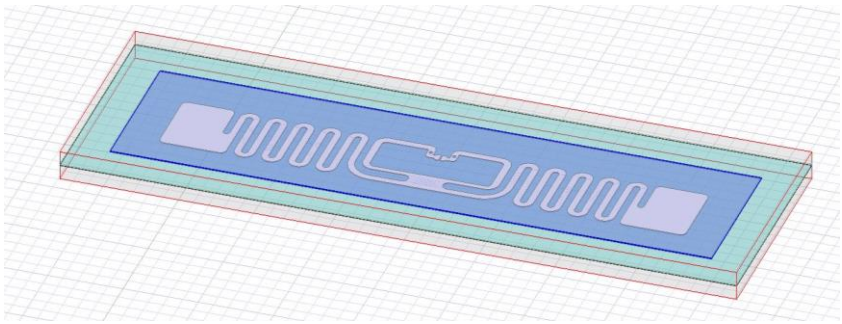

Figure 35. *Heat Simulation in static approach*.

The antenna is placed between two separate stainless-steel blocks (top wall and bottom wall) on a Polyamide “Molded strip”.Since the static and moving walls of the IML machine are both made of steel-type material, stainless steel is chosen for the simulation. The temperature of the top wall is 220°C as the melted plastic, and the bottom wall’s temperature is 40°C like the mold temperature.

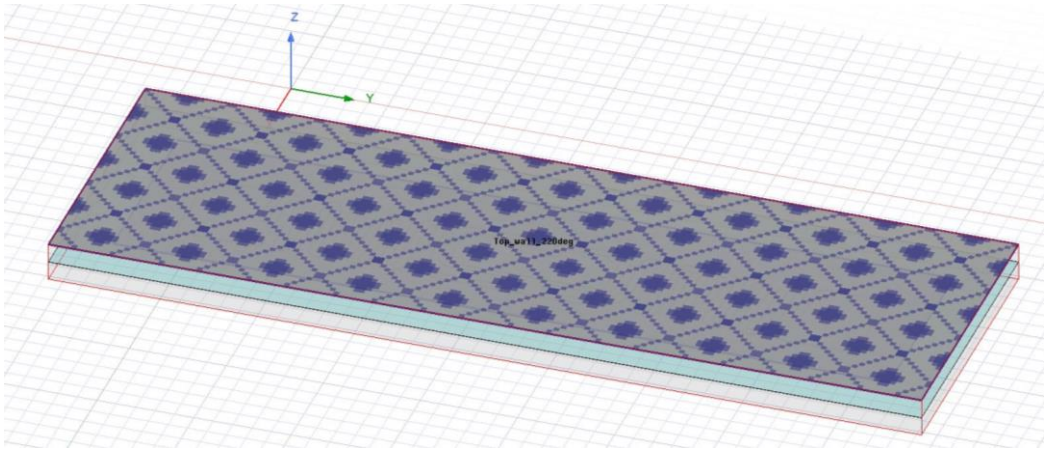

(a)

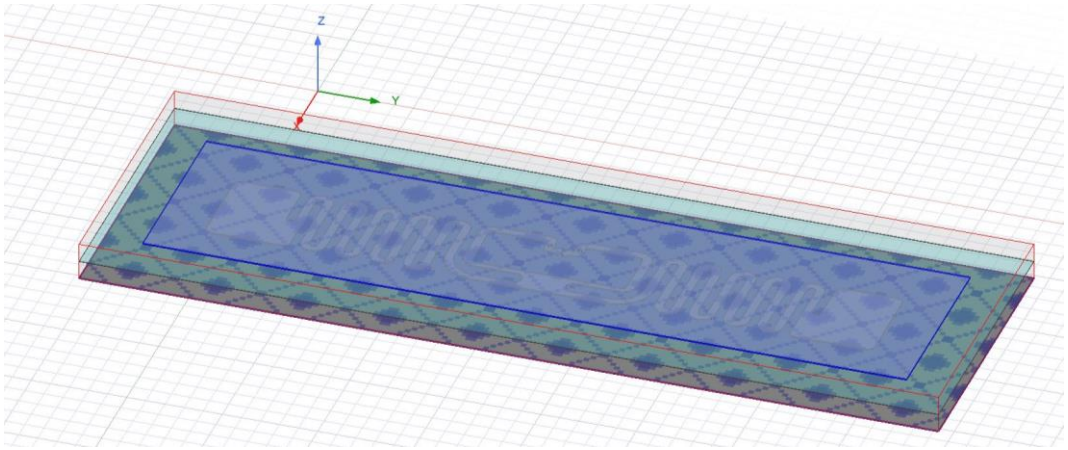

(b)

Figure 36. *IML process in heat simulation; (a) top wall with 220°C, (b) bottom wall of 40°C.*

A cavity (to represent the gap of the mold) was made on the top wall where the Polyamide “Molded strip” (size of 20 mm x 80 mm x 0.15 mm) fully exists and inside it the aluminum antenna (size of 10 mm x 70 mm x 0.1 mm) is placed. The thickness of the aluminum is 9µm. But for a suitable mesh setup, the thickness of the antenna is considered larger than the original (1 mm). The heat simulation is done for antenna 1 with the nominal design and one of the prototypes that do not have any metal in dipole ends except the edge (only 2 mm edge and rest of the part removed from the dipole ends). The motive of selecting this prototype is to observe whether the heat distribution changes according to the presence or absence of metal/ ink in the dipoles.

To make the observation concise, one nominal design and one variant of it is simulated in icepak. As the antenna dimensions are similar, it is considered that the effect of temperature is similar in both designs. Table 2 shows the material properties considered in heat simulation.

Table 2. *Material properties of heat simulation.*

Materials	**Thermal conductivity (W/(m.K))**	**Mass density (Kg/m^3)**	**Thermal expansion coefficient ($10^{-6}/K$)**
Aluminum	237.5	2689	0.233
Polyamide	0.26	0	0
Stainless steel	13.8	8055	0.108

Figure 37 (a) shows the heat distribution of the nominal design of antenna 1 and figure 37 (b) shows the heat distribution of its variant. It is clear that the temperature distribution is uniform in the antenna element, and the surface of the antenna element is more heated than the antenna substrate. Whether there is more amount of metal/ink or not, the heat distribution is similar in both cases. This observation makes a strong agreement in the case of heat distribution with respect to antenna shape or design. Though the simulation scenario is not exactly the same as the practical, yet this observation is considered because of the visual representation of the samples after the IML trials. Some of the samples after IML trials are presented in section 4.3.

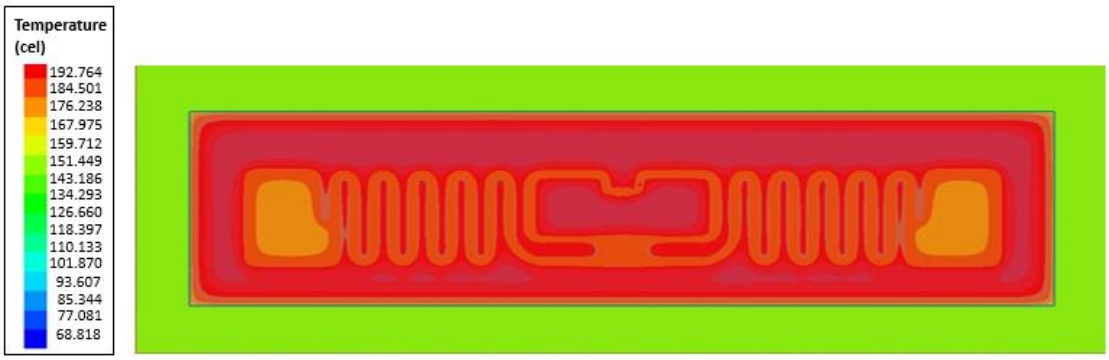

(a)

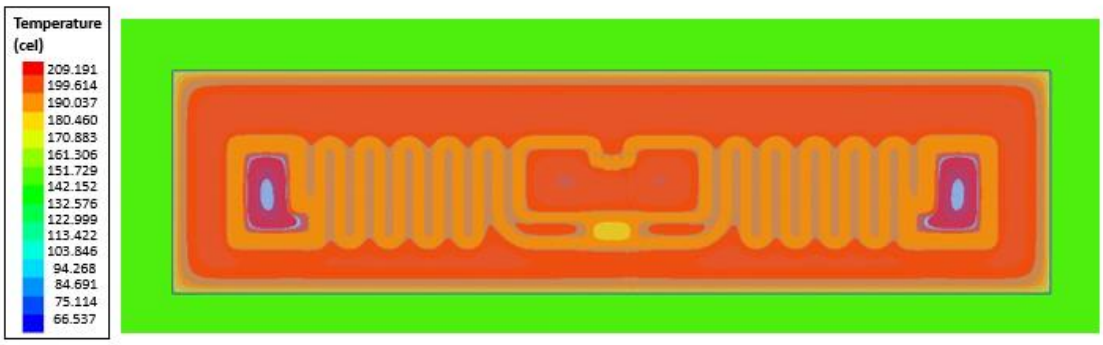

(b)

***Figure 37**. Heat simulation results*

If the heat is distributed uniformly, then there is no effect of changing the shape of antenna to get rid of the wrinkles in resultant sample of IML process. If the antenna element is heated uniformly then it will not vary with the changed design. Indeed, if removing some parts of the antenna does not affect its performance, then it will be very effective in terms of printed antennas. Though for metallic etching, a specific amount of metal will be used anyways; if the antenna is made of conductive ink, then less amount of ink will be utilized, thus making the antenna more environment friendly. For example, in the nominal design of antenna 2 the surface area is 910.26 mm^2, and the circle meshed design is 737.58 mm^2. To find out reduced area percentage the following equation can be utilized,

$$Percentage\_reduction = 100 \times (Area\_original - Area\_mesh)/Area\_original \quad (20)$$

From the equation above, the meshed version of antenna 2 has 19% reduced area. As the amount of ink is proportional to the surface area of the antenna, the amount of ink is also reduced in the meshed version of the antenna with the same performance.

4.3 Visual outcomes

The main objective of this experiment is to achieve an unwrinkled RFID sample going through IML process. Two trials have been done in this objective at Tampere university polymer laboratory with around 100 prototype antennas. In both trials, the results were similar, leading to finding out the reason and solution for the wrinkled IML RFID samples.

To analyze the reason for the wrinkled samples, about 100 types of material were used as the substrate of the antenna and antenna element. All the materials have been printed and etched on the designs discussed above. After the trials, 4 types of cases have been observed from the IML samples, which are as following; in case 1: samples with mesh

designs with wrinkles, case 2: samples with mesh designs without wrinkles, case 3: samples with nominal designs with winkles and case 4: samples with nominal designs without winkles. All the cases are shown in figure; 38, 39, 40 and 41.

Figure 38. *Case 1 contains samples with mesh designs with wrinkles*.

The initial assumption of getting wrinkled or bumped IML RFID was due to uneven heat distribution of the conductive material of the antenna. Therefore the conductive parts have been removed from the antenna without affecting its performance. However, the resultant samples from the IML process do not satisfy the assumption. The bumps or wrinkles still happen to the antennas with less metallic or inked areas.

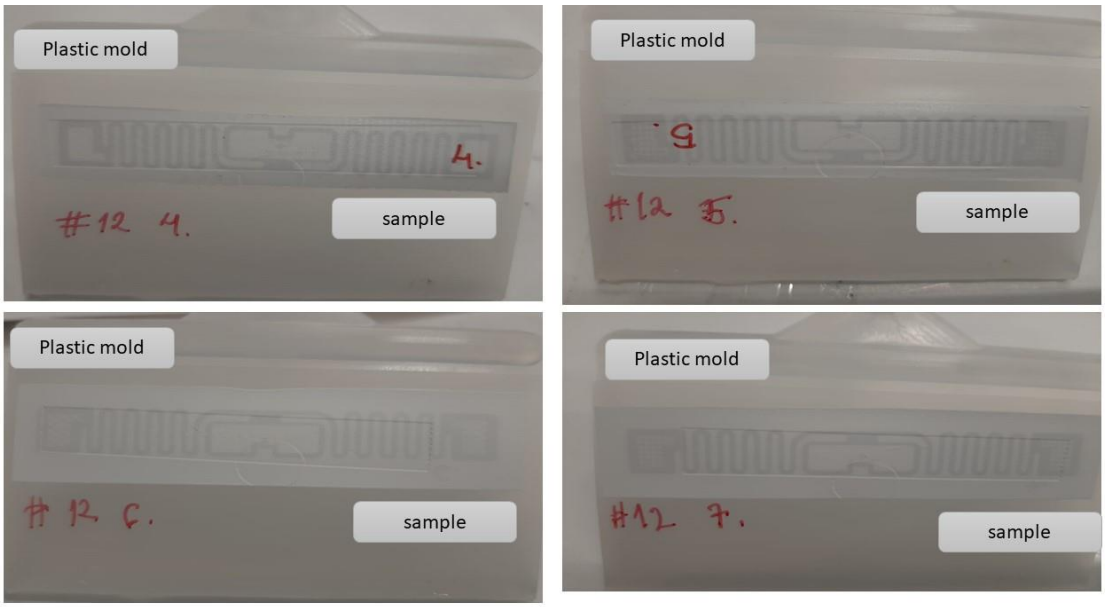

Figure 39. *Case 2 contains samples with mesh designs without wrinkles*.

In both designs (e.g., nominal design or meshed design), some good samples could be achieved from the IML process (in figures 39 and 41). In addition, in both designs, some samples were wrinkled (figures 38 and 40). This means the design does not affect the visual effect of the IML samples. The only fact that can be taken into account is the type of materials that has been used in the antenna. Some good samples were achieved with a few specific materials, which did not have any variation in terms of design.

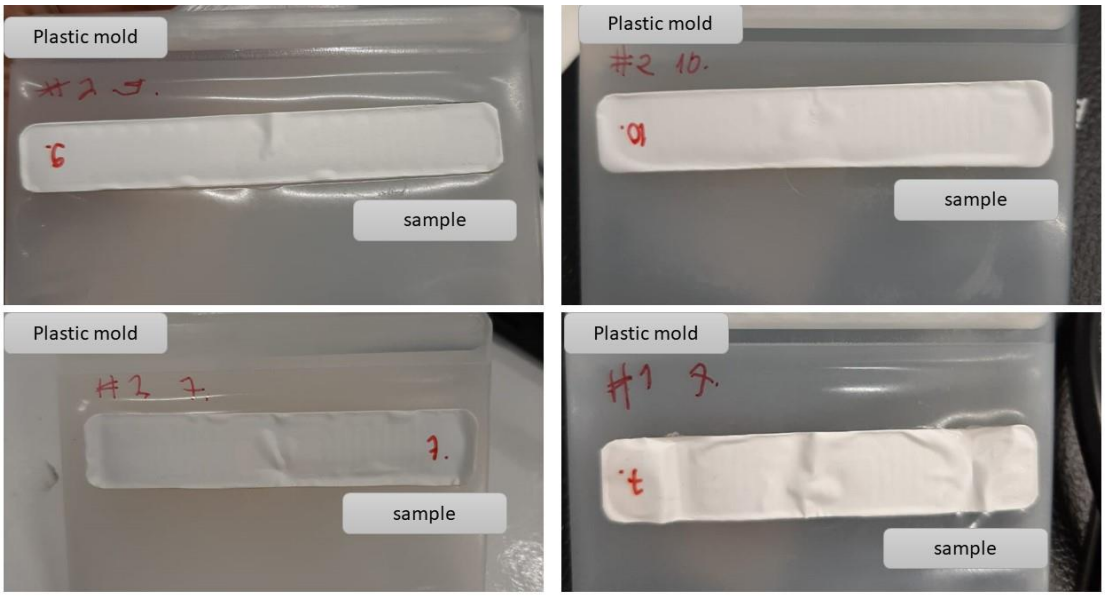

Figure 40. *Case 3 contains samples with nominal designs with wrinkles*.

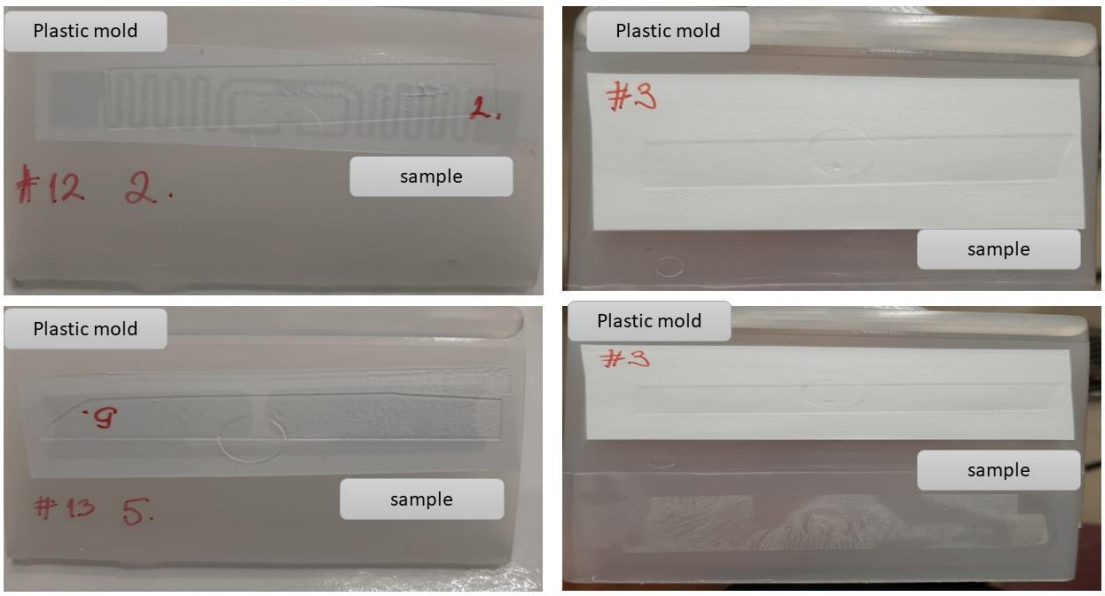

Figure 41. *Case 4 contains samples with mesh designs without wrinkles*.

These observations are very clear to conclude that the wrinkles or bumps happen due to the materials of the antenna, not how it is designed. It depends on the way the materials expand and shrink in the heating and cooling down process in IML. This observation also can be familiarized with the heat simulation results.

There is also a possibility that the size of the IML machine's mold is to blame for the wrinkled samples. It is also possible that because the antenna size is close to the machine's mold size, the melted plastic's edge squeezed the samples in the middle, causing some wrinkles to appear in the core section of the sample.

4.4 Performance analysis of the IML samples

After the IML trials, all the samples were measured again in an anechoic chamber using Voyantic Tagformance UHF tools. The post IML samples were measured to find out:

- Whether both strap attached and direct-attached IC antennas survive through the IML process.
- If they survive, how do they perform after injecting plastic.
- How wrinkles affect the tag’s performance.

Around 100 samples were taken to Tampere university polymer laboratory to observe these phenomena, and there were samples of different materials as antenna elements and substrate. As the ultimate solution to the wrinkling problem depends on the materials, the name of the materials would remain unmentioned in this writing.

The following figures (42, 43, 44) shows 3 types of antenna with different antenna element and polymer substrates.

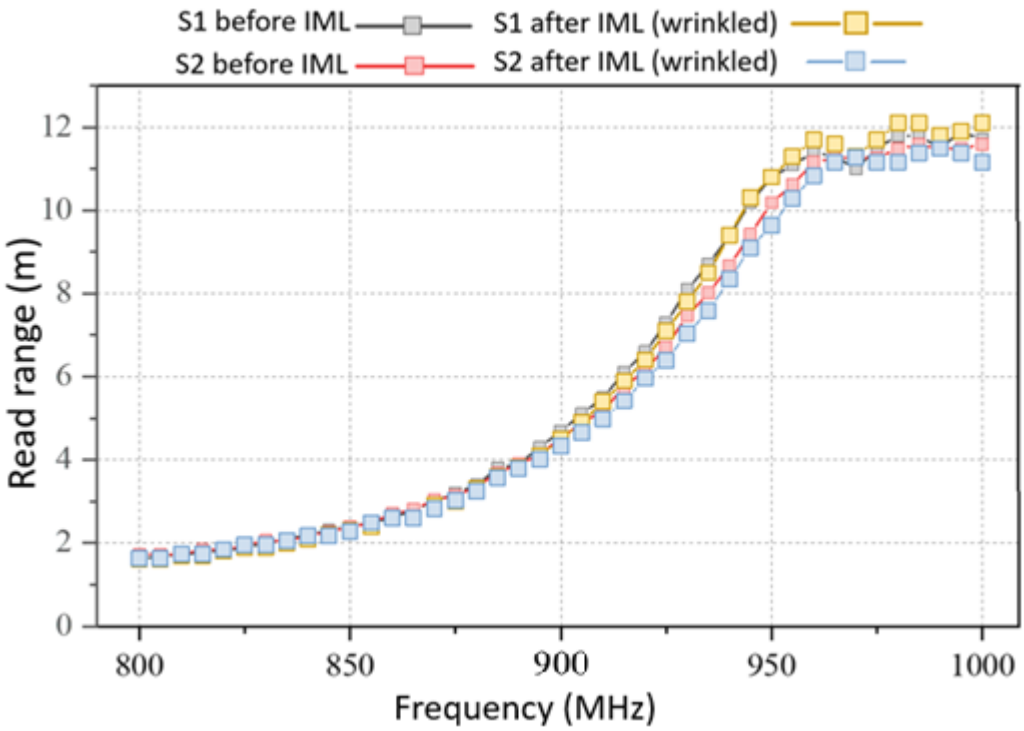

Figure 42. *Type 1 antennas before and after IML*.

The type 1 antennas show that the wrinkled RFID tags after IML perform similarly as before molding. This case signifies that, even though the samples have bumps of wrinkles, they can still function well. Also, a similar case shows in type 2 antennas in figure 43. The wrinkled antennas of type 2 also perform well after molding. The read ranges are different than the measurement results in previous sections because the materials of the antenna and substrates are different and influence the antenna impedance [48].

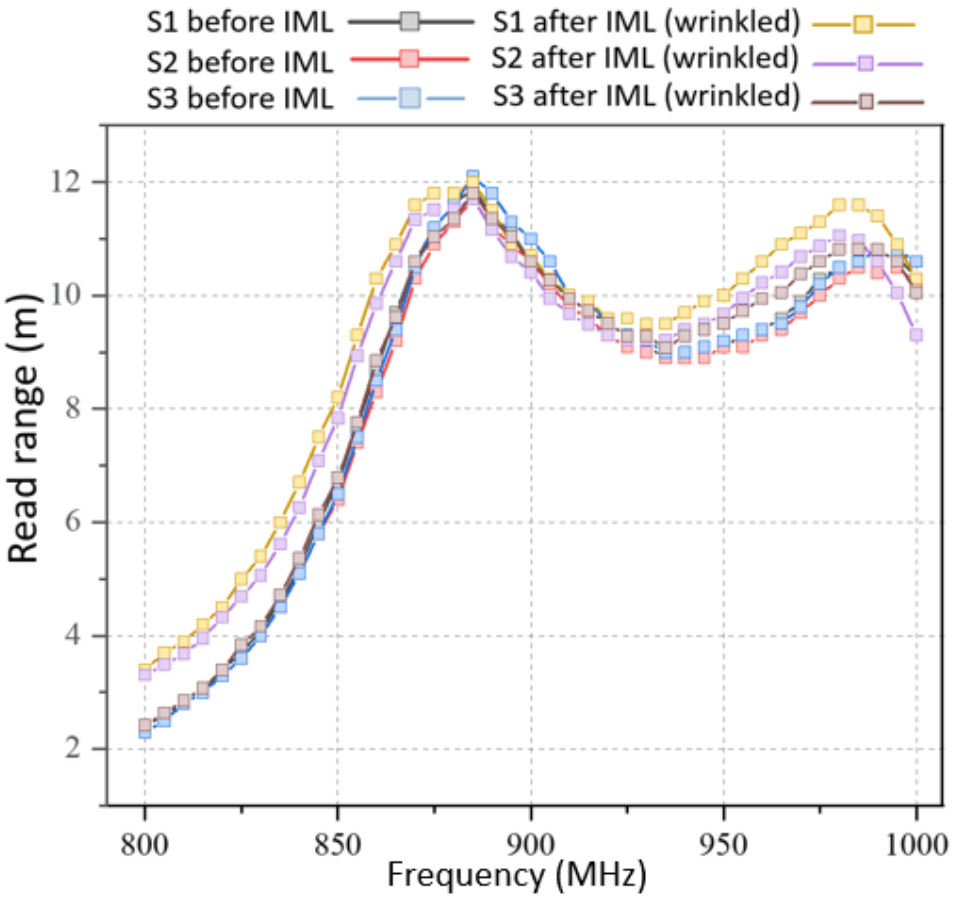

***Figure 43**. Type 2 antennas before and after IML.*

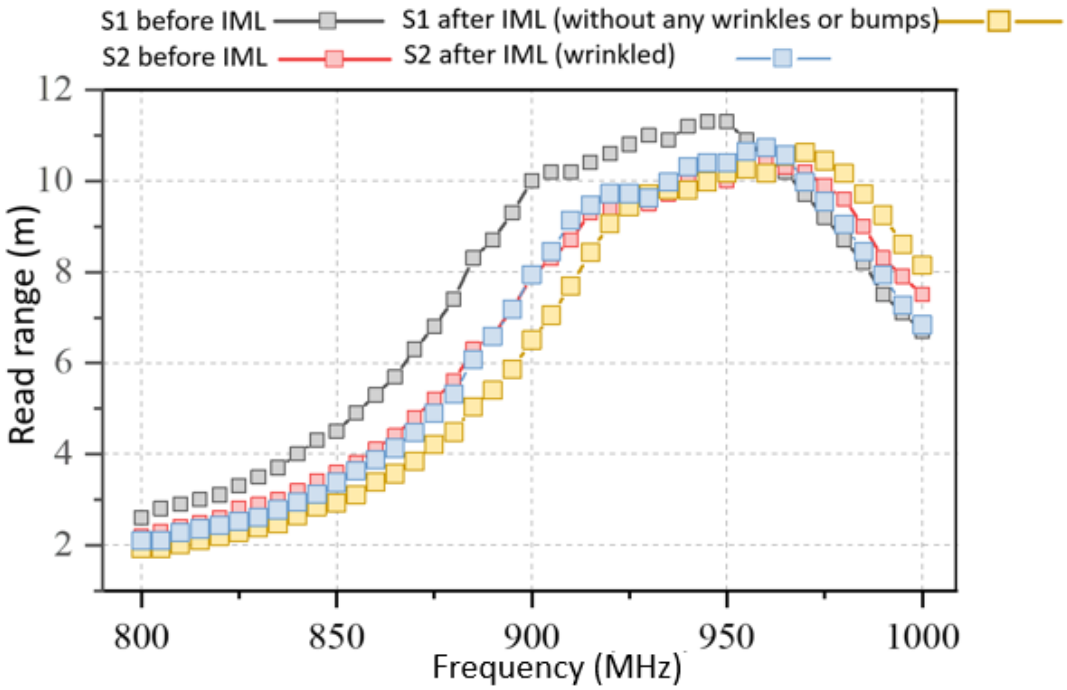

***Figure 44.** Type 3 antennas before and after IML.*

Type 3 shows a precise comparison between wrinkled and unwrinkled IML RFID tags. Both samples with and without wrinkles show similar read ranges after IML compared to the samples before IML process.

Overall, the results presented in this section illustrate that the wrinkles on the samples neither detached the IC (tag is not readable) nor affected the tag's electrical performance in any significant way.

5. CONCLUSION AND FUTURE PERSPECTIVE

5.1 Challenges

The overall work has many segments, and there were different challenges through all the procedures.

- The antenna gets attached with the IC by specific pressure and temperature. As the antennas have a very different combination of materials, the regular temperature and pressure could not be applied. The pressure and temperature were selected in the laminator/bonder according to the materials of the antenna. As there were a lot of samples to prepare, therefore defining correct parameters for each material was very time-consuming.
- As shown in figure 23, the samples for IML process have several layers. Therefore, during the IML process, it was also a challenge how well the layers are attaching.
- Usually, after injecting the plastic, the walls open, and the labeled sample drops down from the mold. Due to using an adhesive layer in the RFID tag, it intends to hold the tag with the mold, which is also a reason for wrinkles or folds on the samples.
- During EM wave simulation, a crucial challenge is balancing simulation time and defining mesh elements for the geometrical structure. As it is discussed in the result section, the approximate results are considered to get the simulation done within a reasonable time (5-6 minutes).

5.2 Future perspective

This study's significant outcome is that the wrinkling problem of IML RFID tags can be solved by choosing the correct materials, and antenna design have no effect on wrinkles. Therefore, the main focus for the future is using specific materials for the antenna on different polymer substrates and developing better results.

As described in section 4.3, the mold size can also be a possible reason for the wrinkled tags; another trial will be done in another machine with a larger mold.

5.3 Conclusion

This thesis considers a very common and crucial problem of IML RFID tags, and possible solutions are analyzed. During IML process, very high temperature melted plastic is injected directly on an RFID tag placed in a mold. The plastic gets cold immediately and becomes the shape of the mold along with the RFID tag. In most cases, the tags get wrinkles or bumps due to this large temperature variation of the process. Sometimes even if the RFID tag is functioning well, the product gets rejected for the outlook.

Initially, it was assumed that the wrinkles occurred due to uneven heat distribution of the melted plastic on the conductive parts of the antenna. Therefore, if the antenna has less conductive materials (metal or ink), the melted plastic would not have large areas to spread on; as a result, the wrinkles might get reduced. However, reducing the antenna element does not refer to decreasing the length of the antenna. By keeping the antenna dimensions the same, the less active radiation parts would be removed so that the performance of the antenna would not be compromised.

The implementation of the initial idea is executed in two Avery Dennison antenna designs. The designs are simulated in HFSS to analyze the current distribution of the antenna, identify its removable parts, and study the EM characteristics. The less active regions of the antenna are removed by using different mesh patterns. In fact, by keeping a reasonable edge of the antenna, the central parts of the dipole ends could be removed completely without hampering the performance as those parts have low current density. Their read ranges compare the performance of the antennas. After applying the mesh patterns or removing the less active parts completely, the variants were selected which have a similar read range as the nominal antennas.

A simple heat simulation is executed in a static environment to observe if the antenna elements show any difference in heat distribution. However, the results showed that the heat distributes on antenna elements uniformly. However, there will be some temperature shock on the antenna surface during the IML trials. Because the liquid spreads gradually from one point to the whole surface of the antenna, it does not spread evenly all over at the same time. But the liquid flow of the plastic was not possible to imitate exactly in simulation.

After preparing the variants of the antennas, the tags are laser etched on metals and printed in flexible conductive inks. The samples are taken to Tampere university polymer laboratory for IML test. After the trials, the IML samples were measured in an anechoic chamber to check whether the samples were functioning optimally.

The overall outcome of this experiment is that the antenna's design does not have any effect on the wrinkling problem of the IML RFID tags. On the other hand, it signifies that the antenna's material is the ultimate solution to this problem.

A very important outcome of this work is also the concept of reducing the metal or ink of the antenna without hampering the antenna performance. Though it does not affect the wrinkling problem of IML process, by using less conductive ink in additive manufacturing of the antenna, it becomes more cost-effective and environment friendly. The experiment will continue with the achieved results and conclusion to develop better IML RFID tags in the future.

REFERENCES

[1] Scanloan, “A Brief History of RFID,” 2003. [Online]. Available: http://www.u.arizona.edu/~obaca/rfid/history.html. [Accessed: 10-Nov-2021]

[2] Panthi, Bikash. “Embedding RFID(Radio Frequency Identification) chip into LPMS(Low Pressure Moulding System) with specific design.” (2013).

[3] A. M. Chalfant, “Embedding Radio Frequency Identification Inlays into Injection Molded Food Containers Using In Mold Labeling Technology,” 2007. [Online]. Available: https://ufdc.ufl.edu/UFE0021620/00001. [Accessed: 10-Nov-2021]

[4] E. Moradi, “Characterization of embroidered dipole-type RFID tag antennas,” 2012 [Online]. Available: https://trepo.tuni.fi/handle/123456789/21061. [Accessed: 24-Nov 2021]

[5] Romagnosi, “A Brief History of RFID,” 2009. [Online]. Available: http://www.u.arizona.edu/~obaca/rfid/history.html. [Accessed: 10-Nov-2021]

[6] “A Brief History of RFID.” [Online]. Available: http://www.u.arizona.edu/~obaca/rfid/history.html. [Accessed: 10-Nov-2021]

[7] Dorman, “A Brief History of RFID,” 2003. [Online]. Available: http://www.u.arizona.edu/~obaca/rfid/history.html. [Accessed: 10-Nov-2021]

[8] Z. Matthias, H. Rupert, S. Simon, W. Valerie, and E. Markus, “Communication with Passive RFID Sensor Tags during Injection Molding of Medical Plastic Parts,” in Smart SysTech 2017-European Conference on Smart Objects, Systems and Technologies, Germany, 2017.

[9] Clampitt, “The RFID Hand Book,” 2006. [Online]. Available: http://rfidhandbook.blogspot.com/2004/11/preface.html. [Accessed: 10-Nov-2021]

[10] S. Lahiri, RFID sourcebook: realistic guidance from an experienced RFID solution architect; learn how to evaluate, plan, and deploy RFID systems. Upper Saddle River, NJ: IBM Press Pearson plc, 2006.

[11] C. Occhiuzzi, S. Caizzone, and G. Marrocco, “Passive UHF RFID antennas for sensing applications: Principles, methods, and classifcations,” IEEE Antennas and Propagation Magazine, vol. 55, no. 6, pp. 14–34, Dec. 2013, doi: 10.1109/MAP.2013.6781700.

[12] "EPCglobal specification for RFID air interface," EPC Radio Frequency Identity Protocols. Class-1 Generation-2 UHF RFID Protocol for Communications at 860 MHz–960 MHz version 1.0.9, January 2005.

[13] S. R. Aroor and D. D. Deavours, “Evaluation of the State of Passive UHF RFID: An Experimental Approach,” IEEE Systems Journal, vol. 1, no. 2, pp. 168–176, Dec. 2007, doi: 10.1109/JSYST.2007.909179.

[14] H. Matsumoto and K. Takei, “An Experimental Study of Passive UHF RFID System with Longer Communication Range,” in 2007 Asia-Pacific Microwave Conference, 2007, pp. 1–4, doi: 10.1109/APMC.2007.4554640.

[15] P. Harrop, “The price sensitivity curve for RFID,” 2006. [Online]. Available: https://www.idtechex.com/. [Accessed: 10-Nov-2021]

[16] Soroka W., 2002, Fundamentals of packaging technology, Institute of Packaging Profes-sionals, Naperville, pp 627.

[17] D. V. Rosato, D. V. Rosato, M. G. Rosato, and D. V. Rosato, Eds., Injection molding handbook, 3rd ed. Boston: Kluwer Academic Publishers, 2000.

[18] Selden R., 2000, “Thin wall molding of engineering plastics,” Journal of Injection Molding Technology, Vol. 4, No. 4, pp. 159-166.

[19] Yao D., and Kim B., 2002, “Increase flow length in thin wall injection molding using rapidly heated mold,” Polymer-Plastics Technology and Engineering, Vol. 41, No. 5, pp. 819- 832.

[20] S. R. Aroor and D. D. Deavours, “Evaluation of the State of Passive UHF RFID: An Experimental Approach,” IEEE Systems Journal, vol. 1, no. 2, pp. 168–176, Dec. 2007, doi: 10.1109/JSYST.2007.909179.

[21] Jechlitschek, Christoph. (2010). A survey paper on Radio Frequency Identification (RFID) trends.

[22] Z. N. Chen and X. Qing, “Antennas for RFID applications,” in 2010 International Workshop on Antenna Technology (iWAT), 2010, pp. 1–4, doi: 10.1109/IWAT.2010.5464865.

[23] Opuchlik M., Jędrasiak K., Cymerski J., Bereska D., Nawrat A. (2018) The Concept of RFID-Based Positioning System for Operational Use. In: Nawrat A., Bereska D., Jędrasiak K. (eds) Advanced Technologies in Practical Applications for National Security. Studies in Systems, De-cision and Control, vol 106. Springer, Cham. https://doi.org/10.1007/978-3-319-64674-9_20

[24] X. Qing, C. K. Goh, and Z. N. Chen, “A Broadband UHF Near-Field RFID Antenna,” IEEE Trans. Antennas Propagat., vol. 58, no. 12, pp. 3829–3838, Dec. 2010, doi: 10.1109/TAP.2010.2078432.

[25] C. A. Balanis, Antenna theory: analysis and design, Fourth edition. Hoboken, New Jersey: Wiley, 2016.

[26] J. Rashed, C.-T Tai, “A new class of resonant antennas,” IEEE Trans. Antennas Propag., vol. 39, pp. 1428-1430, Sep. 1991.

[27] S. R. Best, J. D. Morrow, “On the significance of current vector alignment in establishing the resonant frequency of small space-filling wire antennas,” IEEE Antennas Wireless Propag. Lett., vol. 2, pp. 201-204, 2003.

[28] Sabaawi, Ahmed. (2010). Antennas of RFID Tags.

[29] D. K. Cheng, Field and wave electromagnetics, 2nd edition, Addison-Wesley Publishing Company, Inc. USA, 1992

[30] “Power Density.” [Online]. Available: https://www.phys.hawaii.edu/~anita/new/papers/militaryHandbook/pwr-dens.pdf. [Accessed: 24-Nov-2021] [31] C. A. Balanis, Antenna theory - analysis and design, 3rd edition, John Wiley & Sons, USA, 2005.

[32] D. M. Pozar, Microwave and RF design of wireless systems, John Wiley & Sons, USA, 2001.

[33] A. Lehto, A. Räisänen, Radiotekniikan perusteet, 12th edition, Hakapaino Oy, Helsinki, Finland, 2007

[34] S. R. Saunders, A. Aragón-Zavala, Antennas and propagation for wireless communication systems, 2nd edition, John Wiley & Sons, USA, 2007.

[35] “Wave Polarization and Antenna Polarization.” [Online]. Available: https://www.antenna-theory.com/basics/polarization.php. [Accessed: 10-Nov-2021]

[36] “Polarization and Related Antenna Parameters.” [Online]. Available: https://www.ece.mcmaster.ca/faculty/nikolova/antenna_dload/current_lectures/L05_Polar.pdf. [Accessed: 10-Nov-2021]

[37] M. Schwartz, “Polarization.” [Online]. Available: https://scholar.harvard.edu/files/schwartz/files/lecture14-polarization.pdf. [Accessed: 10-Nov-2021]

[38] J. S. Mandeep and Hilary, “Effects of polarization loss factor, form factors and reader transmitting power on the range of paper and plastic UHF tags in a free and metallic 61 environment,” International Journal of the Physical Sciences, vol. 6(12), no. 18 June, 2011, pp. 2776–2781, Jun. 2011, doi: 10.5897/IJPS11.608.

[39] G. Marrocco, “The art of UHF RFID antenna design: impedance-matching and size reduction techniques,” IEEE Antennas and Propagation Magazine, vol. 50, no. 1, pp. 66–79, Feb. 2008, doi: 10.1109/MAP.2008.4494504.

[40] P. V. Nikitin and K. V. S. Rao, “Antennas and Propagation in UHF RFID Systems,” in 2008 IEEE International Conference on RFID, 2008, pp. 277–288, doi: 10.1109/RFID.2008.4519368.

[41] College of Mechanical and Electrical Engineering, Beijing University of Chemical Technology, Beijing 100029, China et al., “Overview of Injection Molding Technology for Processing Polymers and Their Composites,” ES Mater.Manuf., 2020, doi: 10.30919/esmm5f713. [Online]. Available: http://www.espublisher.com/journals/articledetails/285. [Accessed: 10-Nov-2021]

[42] M. E. Dirckx and D. E. Hardt, “Analysis and characterization of demolding of hot embossed polymer microstructures,” J. Micromech. Microeng., vol. 21, no. 8, p. 085024, Aug. 2011, doi: 10.1088/0960-1317/21/8/085024.

[43] H. Ye, X. Y. Liu and H. Hong, J. Mater. Process. Tech., 2008, 200(1-3), 12-24, doi: 10.1016/j.jmatprotec.2007.10.066.

[44] T. H. Kang, I. K. Kim and Y. S. Kim, Key Engineering Materials, 2006, 306-308, 863-868, doi: 10.4028/0-87849-989- x.863.

[45] V. Radonic, V. Crnojevic-Bengin, and L. Zivanov, “Comparison of Commercially Available Full-Wave EM Simulation Tools for Microwave Passive Devices,” in EUROCON 2005 - The International Conference on “Computer as a Tool,” 2005, vol. 2, pp. 1699–1702, doi: 10.1109/EURCON.2005.1630300.

[46] G. G. Xiao, Z. Zhang, S. Lang, and Y. Tao, “Screen printing RF antennas,” in 2016 17th International Symposium on Antenna Technology and Applied Electromagnetics (ANTEM), 2016, pp. 1–2, doi: 10.1109/ANTEM.2016.7550245.

[47] A. Tomchenko, “The basic screen-printing process.” [Online]. Available: https://www.researchgate.net/figure/The-basic-screen-printing-process_fig1_215521951. [Accessed: 10-Nov-2021]

[48] Datta, Srabanti & Faruk, Md. (2019). Impact of Permittivity and Radiation Pattern on the Performance of a Dipole Antenna. 191-196.

[49] Voyantic, “Tagformance Pro Measurement System Manual.” Voyantic Ltd., 18-Feb-2020.